

# WAIT, WAIT, WAIT...

## WHY DO REASONING MODELS LOOP?

**Charilaos Pipis<sup>\*1</sup>, Shivam Garg<sup>\*2</sup>, Vasilis Kontonis<sup>2</sup>,**  
**Vaishnavi Shrivastava<sup>2</sup>, Akshay Krishnamurthy<sup>2</sup>, Dimitris Papailiopoulos<sup>2, 3</sup>**

<sup>1</sup> MIT    <sup>2</sup> Microsoft Research    <sup>3</sup> University of Wisconsin-Madison

### ABSTRACT

Reasoning models (e.g., DeepSeek-R1) generate long chains of thought to solve harder problems, but they often loop, repeating the same text at low temperatures or with greedy decoding. We study why this happens and what role temperature plays. With open reasoning models, we find that looping is common at low temperature. Larger models tend to loop less, and distilled students loop significantly even when their teachers rarely do. This points to mismatches between the training distribution and the learned model, which we refer to as errors in learning, as a key cause. To understand how such errors cause loops, we introduce a synthetic graph reasoning task and demonstrate two mechanisms. First, risk aversion caused by hardness of learning: when the correct progress-making action is hard to learn but an easy cyclic action is available, the model puts relatively more probability on the cyclic action and gets stuck. Second, even when there is no hardness, Transformers show an inductive bias toward temporally correlated errors, so the same few actions keep being chosen and loops appear. Higher temperature reduces looping by promoting exploration, but it does not fix the errors in learning, so generations remain much longer than necessary at high temperature; in this sense, temperature is a stopgap rather than a holistic solution. We end with a discussion of training-time interventions aimed at directly reducing errors in learning.

### 1 INTRODUCTION

Reasoning models (Jaech et al., 2024; DeepSeek-AI et al., 2025; Abdin et al., 2025; Guha et al., 2025) use extra inference time compute, generating long chains of thought, to solve harder problems. This has opened a complementary scaling axis of inference-time compute, alongside training compute, resulting in striking gains on challenging tasks such as competitive math and coding. Yet these models often get stuck in loops: endlessly repeating the same text in their chain of thought, especially under greedy decoding and low temperatures (see Section 2.1 for an example). As a result, most model providers recommend running them at a sufficiently high temperature to avoid looping (e.g., see the Hugging Face pages for [DeepSeek-R1](#) and [QwQ-32B](#)).

This raises several questions: why do these models loop, and how does temperature help? In particular, does temperature address the root cause or mostly act as a stopgap? Ideally, temperature would be a knob we can use to control how much exploration a chain of thought performs, rather than something we must turn up just to avoid looping. More fundamentally, is randomness a necessary resource for good reasoning models? This is reminiscent of classical questions in algorithms about whether randomized algorithms are more powerful than deterministic ones (Motwani & Raghavan, 1996; Vadhan et al., 2012).

In this work, we take a step towards understanding these questions. Our contributions are as follows.

**Observations with open reasoning models (Section 2).** We evaluate several open reasoning models (e.g., DeepSeek-distilled Qwen, Openthinker-3, Phi-4 reasoning) for looping on problems from the American Invitational Mathematics Examination (AIME), a high-school math contest. We make several observations: (i) all models loop at low temperatures; (ii) within a family, smaller models

---

\*Equal Contribution. Emails: [chpipis@mit.edu](mailto:chpipis@mit.edu), [shigarg@microsoft.com](mailto:shigarg@microsoft.com).

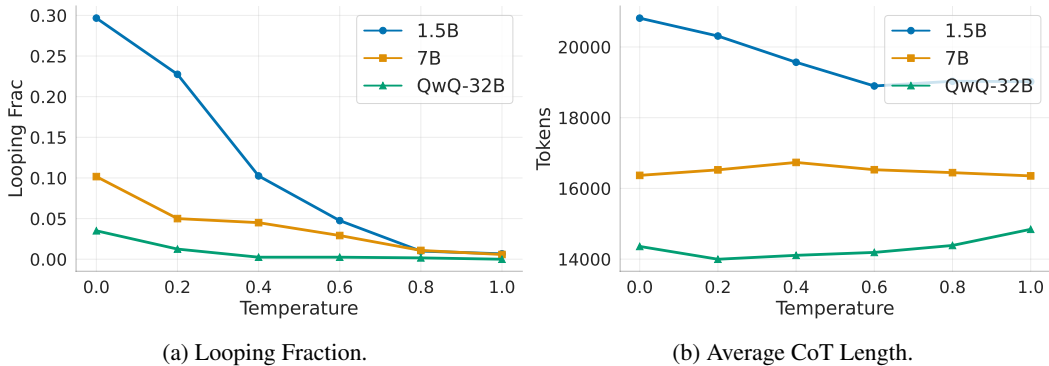


Figure 1: **Looping and response length for OpenThinker model family.** Looping fractions and response lengths for OpenThinker3-1.5B and OpenThinker3-7B (students) and QwQ-32B (teacher), averaged over AIME 2024 and 2025. For each (problem, model, temperature), we generate 20 chains of thought and mark a response as looping if it contains any 30-gram that appears at least 20 times. (a) The smaller student models loop significantly more than the teacher at low temperatures. (b) While increasing temperature largely removes looping for all models, the student models still produce substantially longer responses than the teacher at high temperatures.

loop more; (iii) for models trained via distillation, students loop far more than their teachers; and (iv) for most models, harder AIME problems elicit more looping. These observations point to imperfect learning, that is, systematic *errors in learning* of the training distribution, as a key cause. If a student perfectly learned the teacher, then the amount of looping of the student could not be significantly higher than that of the teacher. For instance (Figure 1), how can it be that OpenThinker3-1.5B loops in 30% of its responses with greedy decoding, while its teacher (QwQ-32B) barely loops?

**Modeling and understanding looping.** Next, building on Bachmann & Nagarajan (2024), we introduce a synthetic graph reasoning task with star graphs to isolate how errors in learning cause looping in a controlled setting. We train Transformers from scratch on random-walk traces that start at a designated start node and aim to reach a leaf goal, mimicking a chain of thought that sometimes makes progress and sometimes backtracks. In this setup we demonstrate two mechanisms through which learning errors cause looping.

*Risk aversion due to hardness of learning (Section 3).* We show that hardness of learning can induce a form of risk aversion. When the correct progress-making action (for example, the next step in a proof) is hard for the model to learn, but an easy cyclic action is available (for example, restating a previously stated fact), the model tends to put relatively more probability on the easy cyclic action, causing looping at low temperatures. We formalize this in Proposition 1, which shows that indistinguishability of the hard action diffuses its probability across many alternatives, while the easy action retains its mass. In our graph reasoning task, this leads to low-temperature loops. Temperature reduces looping and improves accuracy, but the model still assigns too little probability to the progress-making action, so chains at high temperature remain much longer than those of a perfect learner.

*Inductive bias for temporally correlated errors (Section 4).* We also show that even in the absence of hardness of learning, Transformers can have an inductive bias toward looping. When the training distribution places (nearly) equal mass on several progress-making actions at a decision point, small estimation errors tilt the model toward a few options, and these errors are correlated over time. When a similar decision point reappears later in the chain, the model tends to reselect the previously favored actions. Under greedy or low-temperature decoding, these small, temporally correlated errors are amplified and produce loops. We again demonstrate this mechanism in the graph reasoning task, and we observe qualitatively similar patterns in example traces from real reasoning models.

**Role of randomness.** Across these mechanisms, while temperature reduces looping by promoting exploration, it does not fix the underlying errors in learning. As a result, generations at higher temperatures can still be longer than necessary. How effective temperature is depends on the size of these errors. When they are small, as in the temporally correlated errors setting, the increase in response length at high temperature is modest. When they are large, as in the risk-aversion

mechanism, response lengths can be much larger than those of a perfect learner. We see similar behavior in real reasoning models: at higher temperatures, student models such as OpenThinker-3 on average produce longer chains than their teacher. In this sense, randomness or temperature is useful but not a holistic solution.

We end by discussing several promising avenues, including more holistic training-time interventions that directly reduce errors in learning, as well as a better understanding of other forces that contribute to looping (Section 5).

### 1.1 RELATED WORK

While looping has been especially prevalent in *reasoning* models, it has been observed and studied since the early days of large language models (Fan et al., 2018). Holtzman et al. (2020) brought broad attention to this “neural text degeneration,” showing that low-temperature sampling or beam search can yield generic and repetitive text. In response, several mitigations were explored. Unlike-likelihood training explicitly down-weights repeated or undesirable continuations (Welleck et al., 2020), and contrastive methods encourage more isotropic token representations, which reduces repetition (Su et al., 2022). A key data-centric insight was that model repetitions were correlated with repetitions in the training corpus (Li et al., 2023); as instruction-tuning data improved and models scaled, looping became less severe. Consistent with this view, later analyses found that the anisotropy observed in earlier models (e.g., GPT-2) largely disappears in later families such as OPT (Su & Collier, 2023). This aligns with our evaluations as well: we find several instruction-tuned models exhibiting little looping.

With the rise of *reasoning* models, however, severe looping has re-emerged. The very nature of chain-of-thought data, which includes cyclic actions like backtracking and reflection (Li et al., 2025; DeepSeek-AI et al., 2025; Cuadron et al., 2025; Gandhi et al., 2025) provides fertile ground for models to fall into degenerative loops. Moreover, scaling alone is not a satisfactory solution for reasoning models: a core promise of this paradigm is to leverage inference-time compute so that even small models can perform well via longer chains. Understanding and holistically mitigating looping in this setting is therefore important, and our work takes a step towards this.

## 2 OBSERVATIONS ON OPEN MODELS

We conduct a large-scale study of looping on openly available language models. This includes a range of model sizes and training paradigms like distillation from a teacher reasoning model and RL post-training. The reasoning models we tested are as follows. **Qwen:** DeepSeek-R1 Distilled Qwen 1.5B, 7B, 32B (DeepSeek-AI et al., 2025); **Openthinker3:** OpenThinker3 1.5B, 7B (Guha et al., 2025) and QwQ-32B (Team, 2025), which is the teacher for OpenThinker-3 models; **Phi-4:** Phi-4-reasoning, Phi-4-reasoning-plus (Abdin et al., 2025); **Llama:** DeepSeek-R1 Distilled Llama 8B (DeepSeek-AI et al., 2025). While we mostly focus on reasoning models, we also test a few instruction tuned variants (non-reasoning models). These include Qwen2.5-Math-1.5B-Instruct (Yang et al., 2024b), Qwen2.5-1.5B-Instruct (Yang et al., 2024a), Phi-4 (Abdin et al., 2024), Llama-3.1 8B Instruct (Grattafiori et al., 2024)

We consider a text response to contain looping if it contains any  $n$ -gram at least  $k$  times. We choose  $n = 30$  and  $k = 20$  for all reasoning models. Large  $n$  makes it a fairly strict requirement and we observe that qualitative trends are not sensitive to particular choices of  $n$  and  $k$  (see Appendix A.1 for ablations). Additionally, since instruct models produce shorter responses, we relax the looping definition to have  $k = 10$  for them. All plots report averages over AIME 2024 and 2025 (see Appendix A.2 for ablations with GPQA). For each triple (problem, model, temperature) with temperature  $\in \{0, 0.2, 0.4, 0.6, 0.8, 1.0\}$ , we sample 20 responses and compute accuracy, looping percentage, and response length; we then average these quantities across problems.

In Figure 2 we present the looping percentages with greedy decoding for all evaluated models. We show accuracy, looping percentages, and response lengths as a function of temperature for all model families in Appendix A. All open reasoning models we tested loop at low temperature, with looping decreasing as temperature increases. Our main observations are:

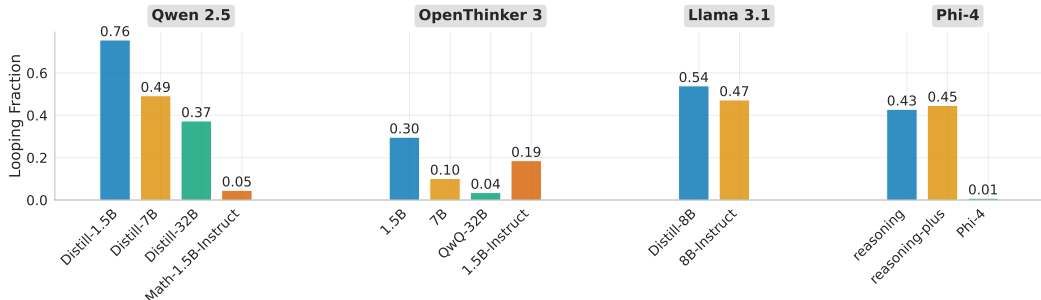


Figure 2: **Looping with greedy decoding.** Bars show the looping fractions at temperature 0, averaged over AIME 2024 and 2025. All reasoning models exhibit looping, and within each family larger models loop less (e.g., Qwen 1.5B > 7B > 32B; OpenThinker3 1.5B > 7B > QwQ-32B). Distilled students can loop significantly more than their teacher (OpenThinker3 vs. QwQ-32B). Reasoning models can also loop heavily even when their instruction-tuned counterparts barely loop (e.g., Qwen2.5 and Phi-4 families). Finally, RL post-training has limited effect on looping in the Phi-4 family (Reasoning vs. Reasoning-Plus).

**Higher capacity models loop less.** Low temperature looping decreases with model capacity (e.g., see the Qwen and OpenThinker-3 families). Further, when distilling from a high-capacity teacher to a low-capacity student, the student can loop significantly more than the teacher (e.g., OpenThinker-3 1.5B vs. QwQ-32B). While looping largely disappears at higher temperatures, higher-capacity models still produce shorter responses (e.g., see Figure 1b). As we will argue in later sections, this phenomenon is closely related to looping.

**Harder problems elicit more looping.** For most models, problems that are harder at high temperature tend to cause more looping at low temperature. Concretely, in each AIME split of 15 problems (AIME-24-I, AIME-24-II, AIME-25-I, AIME-25-II), we rank problems by accuracy at temperature 0.8 and take the easiest 5 and hardest 5. Pooling across the four splits gives 20 easy and 20 hard problems. We then compare the looping rate at temperature 0 on these two groups. For most models, the looping rate is significantly higher on the hard problems than on the easy ones; the only exception is Phi-4 reasoning, which we discuss in Appendix A. This suggests that, no matter how large a model is, there may always exist problems that are hard enough to induce looping, although we leave a more thorough investigation of this conjecture to future work.

**Reasoning models can loop even when their instruct counterparts barely loop.** For the Qwen and Phi-4 model families, we see that the base instruction-tuned models loop very little, while their reasoning counterparts loop a lot. It is not always the case that the instruct models do not loop, as we see with Llama-3.1-8B-Instruct and Qwen2.5-1.5B-Instruct, but even there we observe an increase in the looping percentage for the corresponding reasoning models. The amount a model loops is likely a function of cyclic actions like restatement or backtracking in the training data. This view is supported by past work (Li et al., 2023). We discuss this further in subsequent sections.

**Effect of RL training.** Phi-4 reasoning is one model family where we have access to both a distilled model (Phi-4-Reasoning) and a version that has been lightly tuned with RL (Phi-4-Reasoning-Plus). In this setting, we observe that the looping counts remain roughly the same across the two models.

**What causes looping?** Two patterns stand out in the above observations: low-temperature looping decreases with model capacity, and distilled students can loop far more than their (larger) teachers. If a student perfectly learned its teacher distribution, we would not expect it to loop substantially more than the teacher. The gap thus points to imperfect learning, that is, systematic errors in the learned distribution, as a key cause. The fact that most models loop more on harder problems also aligns with this view. In Sections 3 and 4, we discuss mechanisms through which errors in learning can drive looping. Before that, we go through an example reasoning trace.

## 2.1 AN EXAMPLE TRACE

To get a sense of what happens when models loop, we go through a looping trace generated by OpenThinker-3 1.5B model below.

**Example 1.** The model is prompted to solve Problem I-7 from AIME 2025, with greedy decoding:

The twelve letters  $A, B, C, D, E, F, G, H, I, J, K$ , and  $L$  are randomly grouped into six pairs of letters. The two letters in each pair are placed next to each other in alphabetical order to form six two-letter words, and then those six words are listed alphabetically. For example, a possible result is  $AB, CJ, DG, EK, FL, HI$ . The probability that the last word listed contains  $G$  is  $m/n$ , where  $m$  and  $n$  are relatively prime positive integers. Find  $m + n$ .

The model begins sensibly. It paraphrases the problem and correctly derives the total number of ways to pair up the letters.

First, let me make sure I understand the problem correctly. We have the letters  $A, B, C, D, E, F, G, H, I, J, K$ , and  $L$ . These are to be randomly paired up into six pairs. Each pair is then arranged in alphabetical order to form a two-letter word. Then, all these six words are listed alphabetically. The question is asking for the probability that the last word in this list contains the letter  $G$ .  
...

Let me start with the total number of ways to pair the letters. Since the letters are being paired into unordered pairs, the number of ways to partition 12 letters into 6 pairs is given by  $(12)!$  divided by  $(2^6 * 6!)$ . . . .

Next, it tries to reason about how the two-letter words are formed and loops (semantically) for a bit, repeatedly going over how a word is arranged in alphabetical order.

Now, the next part is figuring out how many of these pairings result in the last word (when the words are listed alphabetically) containing  $G$ . Hmm, so the key here is that the last word in the alphabetically sorted list must contain  $G$ . To do this, I need to think about how the words are formed and how their order is determined.

Each pair is formed by taking two letters and putting them in alphabetical order. So, for any pair, say,  $(X, Y)$ , if  $X$  comes before  $Y$  in the alphabet, then the word is  $XY$ ; otherwise, it's  $YX$ . Wait, but actually, the problem says "the two letters in each pair are placed next to each other in alphabetical order to form six two-letter words". So, regardless of the order in the pair, they are arranged in alphabetical order. So, for any pair, the two letters are ordered such that the first is before the second in the alphabet. Therefore, each pair is effectively an ordered pair in the alphabetical order. So, for example, if the pair is  $(C, D)$ , the word is  $CD$ . If the pair is  $(D, C)$ , the word is  $DC$ , but since they are placed in alphabetical order, it's  $DC$ ? Wait, no, actually, if the pair is  $(D, C)$ , then since  $D$  comes after  $C$ , they would be placed as  $CD$ ? Wait, no, hold on. Wait, the problem says "the two letters in each pair are placed next to each other in alphabetical order". So, regardless of the original order of the pair, they are arranged in alphabetical order. So, for any pair, the two letters are sorted, so the first letter is the earlier one, the second is the later one. So, for example, if the pair is  $(C, D)$ , the word is  $CD$ . If the pair is  $(D, C)$ , the word is  $DC$ . Wait, but actually, the pair is just two letters, so the pair is unordered, but when forming the word, they are arranged in alphabetical order. So, the word is always the two letters in order from  $A$  to  $Z$ . So, the word is the two letters sorted. So, the word is always the first letter being the earlier one, the second the later one. So, the word is the concatenation of the two letters in alphabetical order. So, for any pair, the word is the two letters in order. So, the word is determined by the two letters, but ordered alphabetically. . . .

After this, it briefly comes out of the loop but then slips into another one, now restating the goal of the problem without adding new structure.

Alternatively, maybe it's better to think in terms of the last word in the sorted list. Since the words are sorted alphabetically, the last word is the largest one. So, the problem reduces to: what is the probability that the largest word in the list contains  $G$ ?

Therefore, the problem is equivalent to: when you partition the letters into six pairs, sort each pair into alphabetical order, then sort all the six words alphabetically, what is the probability that the last (i.e., the largest) word contains  $G$ .

Hmm, okay. So, perhaps another way to think about this is: the last word is the maximum of the six words, so the maximum word must contain  $G$ . Therefore, the question is: what is the probability that the maximum word in the set of six sorted pairs is a word that contains  $G$ .

. . . [repeated 2 more times]

Finally, it starts to argue about how pairs including  $G$  can be arranged, but again falls into a loop, repeating that words are formed by sorting the pairs, and never gets out of it.

Alternatively, maybe it's better to think in terms of the possible pairs that include  $G$  and how they can be arranged.

First, let me note that  $G$  is the 7th letter. So, the letters before  $G$  are  $A, B, C, D, E, F$ , and after  $G$  are  $H, I, J, K, L$ . So,  $G$  is in the middle. So, the pairs that include  $G$  can be either  $(G, \text{something before } G)$  or  $(\text{something before } G, G)$ . But when sorted, the pair with  $G$  will be either  $(G, \text{something before } G)$  or  $(\text{something before } G, G)$  but sorted, so it will be  $(\text{something before } G, G)$ . Wait, no. Wait, if the pair is  $(G, H)$ , then the word is  $GH$ . If the pair is  $(H, G)$ , the word is  $HG$ , but since they are sorted, it's  $GH$ . Wait, so actually, the word is always the two letters in alphabetical order, so the word is the pair sorted. Therefore, the word is always the two letters in order, so the word is the same regardless of the original pair. Therefore, the word is determined by the two letters, but sorted. Therefore, the word is the two letters in order. So, the word is the same for any pair of letters, but the pair is unordered. Therefore, the word is the two letters in order. So, the word is the concatenation of the two letters in alphabetical order. Therefore, the word is uniquely determined by the two letters, but the pair is unordered. Therefore, the word is the same for any pair of letters, but the pair is just the two letters. So, the key is that the word is the two letters sorted, so the word is the same as the pair sorted. Therefore, the word is the two letters in order, so the word is the same as the pair sorted. Therefore, the word is the two letters in alphabetical order, so the word is the same as the pair sorted. . . . [keeps repeating the exact same statement]

This trace illustrates a kind of risk-aversion: the model repeatedly takes easy cyclic actions (for example, repeating the same fact about how a two-letter word is formed, or restating the problem), instead of progress-making actions, such as exploring the structural insights needed to solve the problem. An example of structural insight is that for the last word to contain G, no pair should be formed with both letters coming from H-L.

**Further analysis.** To probe this behavior further, we truncate the trace at the point where the final looping begins (right after it says “Wait, so actually, the word is always the two letters in alphabetical order, so the word is the pair sorted.”) and let the teacher model (QwQ-32B) continue from that prefix under greedy decoding. To account for non-determinism, we generate 5 continuations. We get 2 distinct traces: one reaches the correct answer, while the other misses a case and therefore undercounts. However, both traces avoid looping and make significant progress, capturing most of the structural insights. We also regenerate 5 completions from the student model from the same prefix and all of them get stuck in a loop.

To understand how much probability mass the student and teacher put on progress-making actions, we also sample 50 continuations of length 2000 tokens from each model at a high temperature. We then feed these continuations to GPT-5, provide it with a list of key structural insights, and ask whether each continuation contains at least one of them. At temperature 0.7, GPT-5 marks 1/50 student continuations and 34/50 teacher continuations as containing an insight (at temperature 1, these numbers are 8/50 and 32/50). Thus, the student puts much less mass on progress-making actions than the teacher.

Overall, in this example, we see that under greedy decoding the student demonstrates risk-aversion, preferring easy cyclic actions even when the teacher can make progress, and the teacher assigns substantially more probability mass to progress-making actions than the student.

A common behavior across the traces we examined is that of risk-aversion, where the model repeatedly revisits already established facts instead of exploring progress-making actions. In Appendix B, we discuss another trace with a different looping pattern: the model makes a mistake in a proof, develops the argument until it hits a contradiction, then restarts the proof but repeats the same mistake, reaching the same contradiction again, and repeats these series of steps several times.

### 3 RISK-AVERSION DUE TO HARDNESS OF LEARNING

What mechanisms induce risk aversion in models? How do errors in learning cause student models to loop significantly more than their teachers? Understanding these questions is challenging: it requires characterizing the teacher’s data distribution, which can be very complex for real reasoning models, and analyzing how the student modifies this distribution during training, further adding to the complexity. To make progress on these questions, we therefore consider a synthetic graph reasoning setup where we have more control over the data distributions.

We first discuss a mechanism by which hardness of learning can lead to risk aversion and looping, and then describe the graph reasoning task, which we use to instantiate this looping mechanism. For this discussion, it is useful to keep in mind the distillation scenario, where a student model is trained on reasoning chains generated by a teacher (we later discuss how these ideas extend beyond distillation).

As an example, suppose that at some step in the reasoning chain, the teacher’s data distribution has support over two actions: a progress-making action (e.g., the next logical proof step) and a cyclic action (e.g., backtracking or repeating a fact). Assume the progress-making action is hard for the student to learn, while the cyclic action is easy. We show that even if the teacher distribution assigns high probability to the progress-making action, the student can still place relatively more mass on the cyclic action. Thus, while greedy decoding under the teacher distribution would lead to progress, greedy decoding with the student tends to pick the cyclic action repeatedly and get stuck.

The mechanism has two components: (i) a hard-to-learn action co-occurring with an easy action, which increases the easy action’s relative probability and leads greedy decoding to prefer it, and (ii) the easy action being cyclic, which, together with its relatively high probability, causes the model to repeatedly select it. We formalize the hardness of an action below and defer the formalization of cyclic actions to the next subsection, after we introduce the graph reasoning task.

**Formalizing hardness.** We say an action is hard if the model cannot distinguish it from  $n$  other actions. For instance, there may be a natural next step in the proof, but the model confuses it with  $n$  other possibilities. A larger  $n$  corresponds to a harder action. In this case, even if the training distribution assigns high probability to the hard action, the model, trained to maximize log-likelihood, diffuses that mass across the indistinguishable options. The easy action then ends up with relatively higher mass. One way to formalize this is as follows:

**Proposition 1.** Consider the following task: there exist  $n$  sets of contexts  $C_1, \dots, C_n$  which are equi-likely under the training distribution. And there are  $n$  distinct “hard” actions  $a_1, \dots, a_n$ , and an “easy” action  $a_0$ . For every context  $c_i \in C_i$ , the training distribution picks action  $a_i$  with probability  $(1 - p)$  and  $a_0$  with probability  $p$ . Now consider a learner that cannot distinguish between the  $n$  hard actions or, in other words, it is constrained to ignore the context when deciding on the best action. Then the maximum log-likelihood solution for such a learner assigns probability  $p$  to the easy action  $a_0$  and probability  $(1 - p)/n$  to the hard indistinguishable actions  $a_i, \forall i \in \{1, \dots, n\}$ .

We provide the proof in Appendix C. To appreciate the implications, note that as the action becomes harder (i.e., as  $n$  increases), the probability assigned to it decreases as  $(1 - p)/n$ , while the probability of the easy action remains  $p$ . Thus, for sufficiently large  $n$ , greedy decoding picks the easy action.

More generally, whenever the student cannot reliably distinguish an action from several plausible alternatives, maximum-likelihood training encourages it to hedge by spreading probability mass across these candidates. Proposition 1 captures this effect in an extreme case where the hard actions are completely indistinguishable, but the same qualitative behavior can arise whenever the student’s representation collapses many distinct contexts, forcing the model to diffuse probability mass across the actions that are plausible in those contexts. This collapse can arise for several reasons, including limited capacity of the student model or optimization difficulties during training.

**Mapping to language models.** In a language model, an action can be viewed as a short chunk of tokens implementing a logical step (e.g., the next step in a proof). For a span  $x_{t:t+k-1}$ , the model’s probability of that action given the prefix is  $P_\theta(x_{t:t+k-1} | x_{<t}) = \prod_{i=t}^{t+k-1} P_\theta(x_i | x_{<i})$ , so the log-probability of the chunk is the sum of the per-token log-probabilities. Because next-token training maximizes this sum over tokens, it also maximizes the log-probability of any such chunk. Consequently, if a progress-making step is hard (confusable with  $n$  alternative chunks), the model spreads its mass across those chunks, reducing the learned probability on the intended chunk by a  $1/n$  factor, while an easy cyclic span retains its mass. The proposition therefore applies directly to these chunks.

### 3.1 DEMONSTRATION WITH GRAPH REASONING

We demonstrate the looping mechanism discussed above in a synthetic graph reasoning task.

**The star graph.** Our graph reasoning task builds on the hardness result of Bachmann & Nagarajan (2024), who train Transformers to find paths in a star graph. A star graph  $G(n, \ell)$  is a directed graph with a *root*  $r$  and  $n$  simple “spokes,” each a path of length  $\ell - 1$  ending at a distinct leaf (Figure 3). Each training example is a sequence containing the edge list, a start node (the root  $r$ ), a goal node  $g$  (a leaf chosen uniformly at random), and a path from  $r$  to  $g$ . Distinct instances are formed by randomly permuting node labels. Bachmann & Nagarajan (2024) show that Transformers trained with next-token prediction fail to learn the correct path.

Here, aside from the root, all nodes have a single outgoing edge. Thus, for path-finding, learning the first edge on the path is harder than learning the remaining edges. Bachmann & Nagarajan (2024) show that models learn the later edges early in training; once those are learned, the first edge becomes the bottleneck. As a result, the learned solution places roughly  $1/n$  probability on each outgoing edge from the root while predicting subsequent edges correctly, yielding chance accuracy. Recently, Hu et al. (2025) formalized this hardness and showed that, once the easy edges are learned, recovering the right solution is as hard as learning parity, which is conjectured to be hard for gradient-based optimizers (Abbe & Boix-Adsera, 2022; Shalev-Shwartz et al., 2017; Abbe

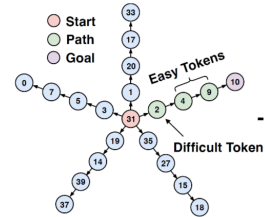
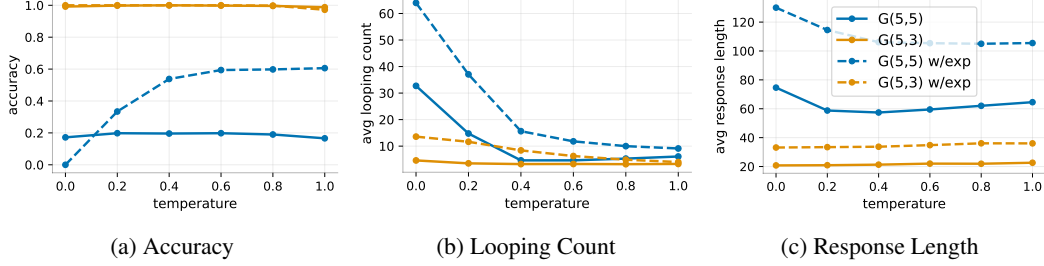


Figure 3: Illustration of star graph. Figure from Bachmann & Nagarajan (2024).

& Sandon, 2023). Note that here the source of hardness is not model capacity (the models have enough capacity to represent the right solution), but the inability of optimization.



**Figure 4: Hard-to-learn actions induce low-temperature loops.** We train small Transformers on random-walk traces on star graphs  $G(5, 5)$  (hard) and  $G(5, 3)$  (easier). In the training distribution, the progress-making action is taken with probability 0.7 and the reset action with 0.3; dashed curves use an exploration variant at the root (0.5 correct edge, 0.2 other children, 0.3 reset). The looping count is the average number of root  $\rightarrow$  start transitions per trace; a perfect learner would have looping count 0 at  $T=0$ . On  $G(5, 5)$ , looping and response length are large at low temperature and decrease with temperature; without exploration, accuracy stays near chance, while with exploration it increases with temperature but is near 0 at  $T=0$ . On  $G(5, 3)$ , looping and response length are small and almost flat, and accuracy is near-perfect for all temperatures. Overall, a hard progress decision at the root, paired with an easy cyclic reset action, drives low-temperature loops, and making the problem easier or adding exploration reduces them.

**The graph reasoning task.** Our graph reasoning task is obtained by making two modifications to the setup of Bachmann & Nagarajan (2024).

*First:* instead of training on a single path from start to goal, we train on a random walk trace that begins at a start node. At any node, the walk moves forward to the next node on the path towards the goal with probability  $1 - p$  and transitions back to the start node with probability  $p$ . For simplicity, we apply this reset from every node, including the start node itself. When  $p = 0$ , this reduces to the original star-graph setting with a single path. We use  $p = 0.3$ .

*Second:* we introduce an explicit start node  $s$  with a single outgoing edge to the root  $r$ . The root and leaf nodes remain as in the standard star graph, and the goal  $g$  is still a leaf. This second modification is not crucial for our results, but it helps illustrate the mechanism better (see observations below). We abuse notation and use  $G(n, \ell)$  to denote this modified star-graph where  $n$  paths of length  $\ell - 1$  emanate from the root, and there exists a separate start node with a single outgoing edge to the root. Finally, in some experiments, we also add a small exploration probability, described later. An example training instance is shown below:

$$\underbrace{11, 16 | 5, 42 | 2, 29 | \dots | 29, 22}_{\text{edge list}} / \underbrace{2, 42}_{\text{start, goal}} = \underbrace{2, 29, 22, 33, 5, 2, \dots, 5, 42}_{\text{random walk}}$$

Each instance is a sequence containing an edge list, a start node, a goal node, followed by a random walk from start to goal. Each node is a separate token, and  $\{\mid, /, =\}$  are separator tokens. As in the original star-graph setting, distinct instances are formed by randomly permuting node labels.

The notions of actions, cyclic actions, and progress-making actions can be precisely stated in this graph reasoning task. An *action* is simply the choice of the next node to visit from the current node. A *cyclic action* is an action that takes the walk to an already visited node, and a *progress-making action* is an action that moves the walk closer to the goal node. In the above task, the teacher distribution takes the progress-making action of moving forward to the next node toward the goal with probability 0.7 and takes a cyclic action (reset to the start) with probability 0.3.

As discussed earlier, for a language model, an action can be viewed as a short chunk of tokens implementing a single logical step in the chain of thought. A cyclic action corresponds to a chunk that repeats something already done before (e.g., restating a previously stated fact), while a progress-making action corresponds to a chunk that moves closer to the final goal (e.g., taking the next step in the proof). Thus if one views the source-to-goal path in the original star-graph setting as a simple

model for the chain of thought of earlier language models that moves toward the goal in a step-by-step manner, then the random-walk variant can be seen as a model for reasoning language models that explore multiple strategies, backtrack, and restart. Our aim, however, is not to capture the full complexity of an actual reasoning model, but to isolate the phenomenon of interest in the simplest setting possible.

**Intuition via a Markovian student.** The random walk defined above only visits nodes along the path from the start to the goal. At each visited node, the training distribution places probability 0.7 on the progress-making action and 0.3 on the cyclic action (reset to the start). A perfect student that exactly recovers this distribution would, under greedy decoding, always take the progress-making action and reach the goal without looping. However, hardness at the root breaks this behavior and induces looping.

The reset action is easy to learn: it only requires reading the start node from context and jumping to it. The progress-making action is also easy at all nodes except the root, where the student must choose among  $n$  outgoing edges. If it cannot distinguish these  $n$  options, we expect it to spread the 0.7 mass on the progress-making action uniformly, assigning  $0.7/n$  to each outgoing edge, while still assigning 0.3 to the easy reset action. At all other nodes, both the progress-making and reset actions are easy, so we expect the student to learn probabilities close to the intended 0.7 and 0.3.

Now suppose that the student is Markovian, so that its next-action distribution depends only on the current node and not on the full history of the walk. Under greedy decoding, the distributions above imply that the walk will loop between the start node and the root: from the start, the student moves to the root, and from the root, whenever  $0.3 > 0.7/n$ , it resets back to the start.

Note that the student does not get trapped in a self-loop at the start node, because both “move to the root” and “stay/reset” there are easy to learn and are assigned probabilities close to 0.7 and 0.3 respectively. Loops arise precisely when a hard action at the root coexists with an easy cyclic action. We introduce the explicit start node in our setup to make this contrast clear.

The above discussion assumes a Markovian student. Transformers, however, are not Markovian as they can condition on the entire prefix. Nevertheless, in the next subsection, we show that similar looping emerges even when the student is a Transformer.

### 3.2 OBSERVATIONS WITH TRANSFORMERS

**Training Details.** We train a decoder-only Transformer from scratch, with 12 layers, 8 attention heads, and 768 embedding dimension ( $\approx 85\text{M}$  parameters). We use Adam for 100k steps with a learning rate of  $10^{-4}$  (cosine decay) and batch size 64. We use 2M training sequences and train with cross-entropy loss for next-token prediction, applying the loss only to the random-walk portion of the sequence. At test time, the model receives new randomly generated instances and, given the edge list, start, and goal, is expected to generate a walk from the start to the goal. We mark a generated walk as accurate if it takes only valid transitions and eventually reaches the goal and stops.

**Low-temperature looping.** We first train the model on the  $G(5, 5)$  graph and do indeed observe looping, similar to the Markovian student discussed above. Figure 4b shows the *average looping count*, defined as the average number of root  $\rightarrow$  start transitions per test instance. The looping count is high at low temperature and decreases as temperature increases. Figure 4c shows that the average response length is also larger under greedy decoding and decreases with temperature. At temperature 0, the looping count is roughly half the response length, since traces often alternate start  $\rightarrow$  root  $\rightarrow$  start  $\rightarrow$  root..., and we count only the root  $\rightarrow$  start transitions. In contrast, a perfect student would have looping count 0 under greedy decoding.

After bouncing between the start node and the root node for a while, the non-Markovian nature of the Transformer kicks in: it eventually commits to a path by choosing one of the outgoing edges from the root and then walking deterministically to a leaf. However, since the model assigns close to uniform probability to all outgoing edges at the root, the chosen leaf is essentially arbitrary. As a result, accuracy remains near chance (Figure 4a).

**Accuracy increases with temperature.** While both looping count and response length drop with temperature, accuracy stays near chance across temperatures. This contrasts with many reasoning models, where accuracy often improves as temperature increases. The difference stems from the training distribution: the walk never explores off-path routes, so the model learns to revisit the *same*

path after each reset. Since it cannot reliably pick the correct path at the root, accuracy remains at chance even when loops shorten.

To test exploration, we modify the walk at the root: with probability 0.3 the walk resets to the start as before, with probability 0.5 it takes the correct outgoing edge (progress-making action), and with probability 0.2 it takes one of the other paths uniformly at random (exploration). At all other non-leaf nodes (out-degree 1), the walk moves forward with probability 0.7 and resets with probability 0.3; it stops at the goal and, upon reaching a non-goal leaf, resets with probability 1. Training on such traces increases accuracy with temperature on  $G(5, 5)$  (w/exp in Figure 4). Interestingly, accuracy at temperature 0 drops near 0: the model tends to bounce between start and root and terminate eventually (e.g., by emitting EOS) rather than committing to a path. Looping count and response length still decrease with temperature, but both are higher than in the non-exploration setting, likely because exploration yields longer training traces and the model mirrors the increase at test time.

**Less looping on easier problems.** We also evaluate  $G(5, 3)$  (with and without exploration). Because the paths from the root to the leaves are shorter, the progress-making action at the root is less hard to learn. Indeed, the learned probabilities place higher mass on the correct outgoing edge from the root than on the others. However, early in generation the model often still prefers the reset at the root over the correct outgoing edge (especially in the exploration variant), so brief looping occurs before it commits to the correct edge and reaches the goal. As a result, accuracy is near perfect across temperatures, and the average response length is essentially stable. This mirrors our earlier finding from Section 2: models loop less on easier problems.

**Overestimation of the reset action.** Our analysis above assumed that, at the root, the student roughly preserves the teacher’s 0.3 probability on the reset action while spreading the remaining 0.7 uniformly over the outgoing edges. In practice, we find that the trained Transformer tends to overestimate the reset probability. For example, on  $G(5, 5)$  with exploration at temperature 0, we examined 500 model-generated trajectories and all positions where the model is at the root. At 94% of these positions, the model assigns more than 0.3 probability to reset, with an average of about 0.35, while still spreading the remaining mass roughly uniformly over the outgoing edges. This further strengthens the dominance of the easy cyclic action and exacerbates looping. A similar overestimation pattern appears on  $G(5, 3)$  and helps explain the brief initial looping observed there, even though the model puts relatively more mass on the correct outgoing edge from the root than on the others. We hypothesize that this overestimation bias arises from the prevalence and ease of learning of the reset action, but leave a more thorough analysis to future work.

### 3.3 OTHER IMPLICATIONS

**Sources of hardness.** In the illustration above, hardness comes from the inability of the optimization to find the right solution. More generally, hardness can arise due to other factors too such as limited model capacity or limited training compute (under-training). The hardness due to model capacity is a plausible explanation for why smaller models loop more within a family trained on the same data.

**Temperature as a mitigation.** In the beginning, we asked whether temperature is a stopgap or a holistic fix. The above analysis suggests an answer. While increasing temperature reduces looping and improves accuracy, it does not remove the underlying learning errors: the model still assigns too little probability to the correct progress-making action. A simple diagnostic is the response length at high temperature. On  $G(5, 5)$  with exploration, the learned model at temperature 1 produces responses with an average length of 105.5, whereas a perfect learner would have an average length of 24.8, more than four times shorter. Thus, higher temperature helps by encouraging exploration, but it does not correct the learning errors, and the generations remain much longer than necessary. This also explains our observation with open reasoning models: even at higher temperatures, smaller reasoning models tend to produce longer chains than larger models or their teachers. More holistic fixes would require training-time interventions; we return to these in Section 5.

**Instruct vs Reasoning Models.** Two ingredients are needed in the mechanism above: (i) hard-to-learn actions, along with (ii) easy-to-learn cyclic actions present in the training distribution. The presence of hard actions amplifies the frequency of easy cyclic actions in model generations. However, if cyclic actions are rare in the training traces, extensive looping is less likely. This is a plausible explanation for why many instruction-tuned models loop less than reasoning models as reasoning traces include more cyclic actions such as re-statement and backtracking.

**RL vs distillation.** The mechanism discussed in this section can affect models trained via RL too, and not just distillation. A guiding principle here is that whenever there is a capacity difference between the teacher model and the student model, hardness of learning for the student can amplify looping behavior. One can approximately view the RL training process as sampling multiple trajectories from the model and training on the correct ones. While there is no explicit teacher model for a RL trained model, this can be thought of as training the model on best-of- $k$  version of itself where  $k$  is the number of trajectories sampled. In that sense, there is still a gap between the data generator and the learner, which can possibly cause this mechanism.

## 4 AN INDUCTIVE BIAS FOR LOOPING

In this section, we show that Transformers can have an inductive bias for looping even in the absence of any hardness in learning. The mechanism is easiest to describe in the graph reasoning setting, so we directly jump in.

**Setup.** We use the same star graph as in Section 3 (including the start node), but change the random walk. The walk begins at the start node. At each non-leaf node, it chooses one outgoing edge uniformly at random. Thus all non-root internal nodes (out-degree 1) always take their unique outgoing edge, while the root chooses uniformly among its  $n$  children. If the walk reaches the goal (a leaf), it stops; if it reaches a non-goal leaf, it transitions back to the start. Note that, unlike the previous section, there is no hardness at the root node here, as the walk simply chooses a child uniformly at random. We train Transformers on traces drawn from this process; training and test details match the previous section.

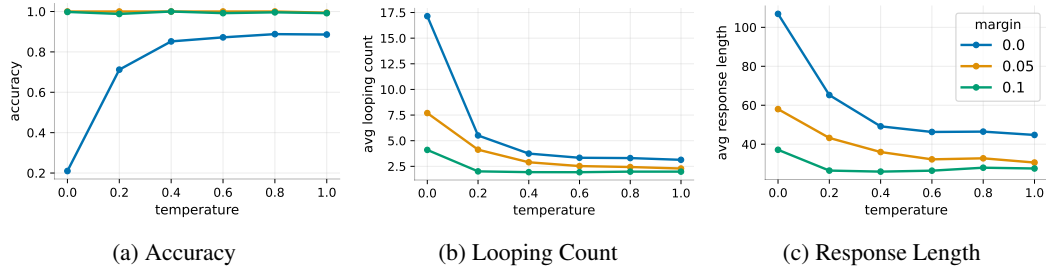


Figure 5: **Temporally correlated errors induce low-temperature loops.** We train on  $G(5, 5)$  star-graph random-walk traces that choose a child at the root, take the unique outgoing edge at other internal nodes, and reset to the start at non-goal leaves. For  $m=0$ , the training walk always chooses a root child uniformly at random; for  $m>0$ , a margin biases the walk toward children that have not yet been visited. The trained models develop *temporally correlated* errors at the root, repeatedly selecting the same few children at low temperatures and thus looping; this effect is weakened, but not removed, by the margin. (a) Accuracy: near chance for  $m=0$  at low temperature and increasing with temperature; margin variants achieve near-perfect accuracy across temperatures. (b) Looping count: for each trace, we count visits to each root child and take the maximum, then average over test instances. Lower temperatures have higher looping counts; margins reduce them. (c) Response length: longer at lower temperatures, and shortened by margins.

### 4.1 OBSERVATIONS AND IMPLICATIONS

**Low temperature loops.** It helps to first consider a perfect learner. On  $G(n, \ell)$ , such a model would learn: probability 1 to the unique outgoing edge at non-root internal nodes; probability 1 to reset at non-goal leaves; and probability  $1/n$  to each child at the root. In practice, the trained model deviates slightly at the root. Instead of learning an exact  $1/n$  split, it makes small errors (e.g.,  $0.2 \pm 0.05$  for  $n=5$ ). More importantly, these errors are *correlated across time*: the root children that are slightly preferred early in the trace tend to remain preferred on later visits to the root. Under greedy decoding or low temperature, the model therefore keeps revisiting the same one or two paths, producing loops.

We quantify this with a *looping count*: for each generated trace, we record how many times each root child is visited and report the maximum over children; we then average this value over 500 test instances. In Figure 5 (margin = 0), we show the accuracy, looping count and average response length versus temperature for a model trained on  $G(5, 5)$ . We observe that the looping count is high

at low temperature and decreases as temperature increases. The average response length shows the same trend. Accuracy is near chance at temperature 0 and improves with temperature.

**Temporal correlation.** In addition, we directly probe temporal correlation in the model’s predictions at the root. Across test instances, we measure two quantities. For each generated trace, we look at every pair of *consecutive* visits to the root and, for each pair, we find the two children with the highest probabilities. We then compute (i) the fraction of such consecutive-visit pairs where the child with the highest probability is the same at both visits, and (ii) the analogous fraction for the child with the second-highest probability. These fractions are 96.7% and 76.7%, respectively—far higher than one would expect if predictions on consecutive visits were uncorrelated. Thus the Transformer’s errors at the root are temporally correlated, inducing an inductive bias for looping.

**A variant with margins.** The training walk above samples root children uniformly at every visit. What if the training distribution itself discourages revisiting already-seen children? We study a *margin* variant: the first time the root is visited, a child is sampled uniformly; on later visits, each child that has ever been visited at the root has its sampling probability reduced by a fixed margin  $m$ , and the removed mass is redistributed uniformly over the as-yet-unvisited children. This reduction is applied once per child (its probability does not decrease further with repeated visits). Note that with  $m=0$  we recover the random walk considered above, and for  $m>0$  the process is no longer Markovian.

Training with  $m=0.05$  and  $m=0.1$  reduces low-temperature looping counts and response lengths compared to  $m=0$ , and accuracy becomes near-perfect across temperatures (Figure 5). Temporal correlation at the root, as measured by the consecutive-visit fractions above, also weakens: for  $m=0.05$ , the child with highest probability is the same across consecutive visits 77.1% of the time and the second-highest child is the same 53.7% of the time; for  $m=0.1$ , these fractions drop to 61.6% and 48.0%, respectively (versus 96.7% and 76.7% when  $m=0$ ). However, these correlations are still substantial: under the margin-modified training distribution, a perfect student decoded greedily would never revisit an already-visited child at the root, so the fraction of consecutive visits on which the same child has the highest probability would be zero.

There are two ways to interpret the margin variant results. On one hand, they show the robustness of the looping mechanism: the student still over-prefers already-visited children even when the training distribution nudges it away. On the other hand, they suggest a mitigation: biasing traces toward new actions reduces looping. While this is a training-time intervention in our experiments, existing inference-time interventions that explicitly discourage repetition are in a similar vein (Keskar et al., 2019).

**Example trace.** The mechanism above illustrates that a Transformer can have a bias toward repeating its errors. In Appendix B, we show an example looping trace from OpenThinker3-1.5B that exhibits a similar pattern. In that trace, the model makes a mistake at some point in the proof, continues to develop the argument until it reaches a contradiction, then restarts the proof but repeats the same mistaken step, hits the same contradiction again, and loops through this sequence multiple times. In our graph reasoning task, this is analogous to repeatedly choosing the same incorrect child at the root, following the corresponding path to a leaf, restarting, and looping through the same set of nodes.

**Comparing the two mechanisms.** Both looping mechanisms we discuss stem from errors in learning, but they differ in nature. The first arises from *hardness of learning*: probability mass on a hard progress-making action is diffused across many indistinguishable alternatives. Importantly, this gap can be large relative to the training distribution and does not rely on Transformer-specific inductive biases—it appears for any maximum-likelihood learner when the correct action is indistinguishable from many others. The second relies on an *inductive bias toward temporally correlated errors*: the learned probabilities at repeated decision points are slightly but consistently skewed toward a few actions. Here the deviations are small, yet sufficient for greedy/low-temperature decoding to loop.

These two mechanisms can also be viewed as two atomic “forces” driving looping. In Appendix D, we present a variant where they act together: the training distribution already places significantly more mass on the child leading to the goal (rather than a uniform  $1/n$  split), but hardness of learning prevents the student from fully exploiting this advantage, and its errors at the root remain temporally correlated. As a result, the model still demonstrates looping even though the training distribution strongly favors the correct action.

**Temperature as a mitigation.** In Section 3, we saw that temperature mainly helps by promoting exploration, but cannot fix the underlying learning errors; as a result, generations at high temperature remained much longer than necessary (on  $G(5, 5)$  with exploration, the learned model at temperature 1 had average length 105.5 versus 24.8 for a perfect learner, a  $\approx 4\times$  blowup). In the present setting, the learning errors are smaller: the model’s distribution at the root is already close to the ideal (roughly uniform over children), with only mild skew that creates temporally correlated loops. Repeating the same diagnostic here, on  $G(5, 5)$  with margin = 0 at temperature 1, the learned model has average response length 44.7 compared to 27.7 for the perfect learner ( $a \approx 1.5\times$  blowup). This contrast suggests that temperature is a reasonably effective fix when the learning errors are small, whereas when the errors are large, more holistic training-time interventions might be better.

**A catalyst for looping.** In looping traces with open reasoning models, we also see another interesting phenomenon. At the beginning of a loop, the model’s probability distribution over next tokens looks relatively normal, but as it repeats the same text, it becomes increasingly confident (Appendix E). This acts as a catalyst for any looping mechanism, making it harder for the model to escape once it has been looping for a while. This behavior has also been observed in prior work for earlier generation of language models (Holtzman et al., 2020; Chiang & Chen, 2021; Xu et al., 2022). One possible explanation for this bias is that pretraining data may contain some repeated sequences. So once the model has repeated something several times, the most likely continuation conditioned on this history is to repeat further. Understanding the sources of this bias more precisely is an interesting direction for future work. In Appendix E, we explicitly introduce such a bias into our trained models and show that it amplifies the looping mechanisms discussed above.

## 5 DISCUSSION

We began with the question: why do reasoning models loop, and is randomness (temperature) a holistic fix or a stopgap? Our evaluation of open reasoning models points to errors in learning as a key cause. Using a synthetic graph reasoning task, we then highlighted two natural mechanisms through which learning errors can cause looping: risk aversion caused by hardness of learning, and an inductive bias toward temporally correlated errors.

On the role of randomness, we found that temperature is reasonably effective at decreasing looping, but it cannot fix the underlying learning errors: the model can still assign too little probability to the correct progress-making actions. As a result, response lengths at high temperature remain longer than necessary. Thus temperature is a reasonable fix when the errors are small (as in the temporally correlated errors mechanism), but is more of a stopgap when they are large (as in the hardness-based mechanism).

**Beyond temperature.** A natural next step is to look for holistic fixes that directly reduce errors in learning. Some errors made by small models are inevitable, since capacity is a bottleneck, but it is unlikely that all of the errors we see today are necessary. One concrete direction is to modify how we distill teacher traces into a student: instead of training directly on the raw traces, we can try to make them easier for the student to learn. For example, a targeted data augmentation approach could identify points in teacher traces that the student finds hard (e.g., high-loss positions) and augment them with brief hints. Other levers include better curricula and architectures to mitigate hardness-based errors (e.g., for star-graph style hardness, recent work shows that newer architectures can help (Hu et al., 2025; Ahn et al., 2025)).

**Other forces at play.** Our synthetic graph reasoning task is intentionally simple, designed to isolate some natural mechanisms behind looping. While we do see glimpses of these mechanisms in real traces, language models are much more complex, and other forces beyond what we study here likely also contribute. One force that is worth investigating more is error accumulation: errors made during generation compound over time. The mechanisms we propose show that looping can arise even without such accumulation. But in practice error accumulation may act as a catalyst. For example, one instance of error accumulation we discuss is that once the model starts repeating a sequence, the repetition reinforces itself and becomes harder to escape (see Appendix B for another example trace where we discuss how error accumulation could play a role). Past work has also noted that looping sequences are often preceded by less natural text, which is consistent with error accumulation playing a role (Chiang & Chen, 2021). Understanding the precise mechanisms by

which error accumulation contributes to looping (e.g., using controlled setups similar to ours) is a worthwhile direction for future work.

In summary, our work takes a step toward a better understanding of looping in reasoning models by surfacing a few natural mechanisms and studying them in a controlled setting. We hope it provides a useful foundation for exploring other factors that contribute to looping and for developing more holistic mitigation strategies in future models.

## REFERENCES

- Emmanuel Abbe and Enric Boix-Adsera. On the non-universality of deep learning: quantifying the cost of symmetry. *Advances in Neural Information Processing Systems*, 35:17188–17201, 2022.
- Emmanuel Abbe and Colin Sandon. Polynomial-time universality and limitations of deep learning. *Communications on Pure and Applied Mathematics*, 76(11):3493–3549, 2023.
- Marah Abdin, Jyoti Aneja, Harkirat Behl, Sébastien Bubeck, Ronen Eldan, Suriya Gunasekar, Michael Harrison, Russell J. Hewett, Mojan Javaheripi, Piero Kauffmann, James R. Lee, Yin Tat Lee, Yuanzhi Li, Weishung Liu, Caio C. T. Mendes, Anh Nguyen, Eric Price, Gustavo de Rosa, Olli Saarikivi, Adil Salim, Shital Shah, Xin Wang, Rachel Ward, Yue Wu, Dingli Yu, Cyril Zhang, and Yi Zhang. Phi-4 technical report, 2024. URL <https://arxiv.org/abs/2412.08905>.
- Marah Abdin, Sahaj Agarwal, Ahmed Awadallah, Vidhisha Balachandran, Harkirat Behl, Lingjiao Chen, Gustavo de Rosa, Suriya Gunasekar, Mojan Javaheripi, Neel Joshi, Piero Kauffmann, Yash Lara, Caio César Teodoro Mendes, Arindam Mitra, Besmira Nushi, Dimitris Papailiopoulos, Olli Saarikivi, Shital Shah, Vaishnavi Shrivastava, Vibhav Vineet, Yue Wu, Safoora Yousefi, and Guoqing Zheng. Phi-4-reasoning technical report, 2025. URL <https://arxiv.org/abs/2504.21318>.
- Kwangjun Ahn, Alex Lamb, and John Langford. Efficient joint prediction of multiple future tokens. *arXiv preprint arXiv:2503.21801*, 2025.
- Gregor Bachmann and Vaishnav Nagarajan. The pitfalls of next-token prediction. In Ruslan Salakhutdinov, Zico Kolter, Katherine Heller, Adrian Weller, Nuria Oliver, Jonathan Scarlett, and Felix Berkenkamp (eds.), *Proceedings of the 41st International Conference on Machine Learning*, volume 235 of *Proceedings of Machine Learning Research*, pp. 2296–2318. PMLR, 21–27 Jul 2024. URL <https://proceedings.mlr.press/v235/bachmann24a.html>.
- Vidhisha Balachandran, Jingya Chen, Neel Joshi, Besmira Nushi, Hamid Palangi, Eduardo Salinas, Vibhav Vineet, James Woffinden-Luey, and Safoora Yousefi. Eureka: Evaluating and understanding large foundation models. *Microsoft Research. MSR-TR-2024-33*, 2024.
- Vidhisha Balachandran, Jingya Chen, Lingjiao Chen, Shivam Garg, Neel Joshi, Yash Lara, John Langford, Besmira Nushi, Vibhav Vineet, Yue Wu, and Safoora Yousefi. Time scaling for complex tasks: Where we stand and what lies ahead. *Microsoft Research. MSR-TR-2025-16*, 2025.
- Ting-Rui Chiang and Yun-Nung Chen. Relating neural text degeneration to exposure bias. *arXiv preprint arXiv:2109.08705*, 2021.
- Alejandro Cuadron, Dacheng Li, Wenjie Ma, Xingyao Wang, Yichuan Wang, Siyuan Zhuang, Shu Liu, Luis Gaspar Schroeder, Tian Xia, Huanzhi Mao, Nicholas Thumiger, Aditya Desai, Ion Stoica, Ana Klimovic, Graham Neubig, and Joseph E. Gonzalez. The danger of overthinking: Examining the reasoning-action dilemma in agentic tasks, 2025. URL <https://arxiv.org/abs/2502.08235>.
- DeepSeek-AI, Daya Guo, Dejian Yang, Haowei Zhang, Junxiao Song, Ruoyu Zhang, Runxin Xu, Qihao Zhu, Shirong Ma, Peiyi Wang, Xiao Bi, Xiaokang Zhang, Xingkai Yu, Yu Wu, Z. F. Wu, Zhibin Gou, Zhihong Shao, Zhuoshu Li, Ziyi Gao, Aixin Liu, Bing Xue, Bingxuan Wang, Bochao Wu, Bei Feng, Chengda Lu, Chenggang Zhao, Chengqi Deng, Chenyu Zhang, Chong Ruan, Damai Dai, Deli Chen, Dongjie Ji, Erhang Li, Fangyun Lin, Fucong Dai, Fuli Luo, Guangbo Hao, Guanting Chen, Guowei Li, H. Zhang, Han Bao, Hanwei Xu, Haocheng Wang, Honghui Ding,

Huajian Xin, Huazuo Gao, Hui Qu, Hui Li, Jianzhong Guo, Jiashi Li, Jiawei Wang, Jingchang Chen, Jingyang Yuan, Junjie Qiu, Junlong Li, J. L. Cai, Jiaqi Ni, Jian Liang, Jin Chen, Kai Dong, Kai Hu, Kaige Gao, Kang Guan, Kexin Huang, Kuai Yu, Lean Wang, Lecong Zhang, Liang Zhao, Litong Wang, Liyue Zhang, Lei Xu, Leyi Xia, Mingchuan Zhang, Minghua Zhang, Minghui Tang, Meng Li, Miaojun Wang, Mingming Li, Ning Tian, Panpan Huang, Peng Zhang, Qiancheng Wang, Qinyu Chen, Qiushi Du, Ruiqi Ge, Ruisong Zhang, Ruizhe Pan, Runji Wang, R. J. Chen, R. L. Jin, Ruyi Chen, Shanghao Lu, Shangyan Zhou, Shanhuang Chen, Shengfeng Ye, Shiyu Wang, Shuiping Yu, Shufeng Zhou, Shuting Pan, S. S. Li, Shuang Zhou, Shaoqing Wu, Shengfeng Ye, Tao Yun, Tian Pei, Tianyu Sun, T. Wang, Wangding Zeng, Wanjia Zhao, Wen Liu, Wenfeng Liang, Wenjun Gao, Wenqin Yu, Wentao Zhang, W. L. Xiao, Wei An, Xiaodong Liu, Xiaohan Wang, Xiaokang Chen, Xiaotao Nie, Xin Cheng, Xin Liu, Xin Xie, Xingchao Liu, Xinyu Yang, Xinyuan Li, Xuecheng Su, Xuheng Lin, X. Q. Li, Xiangyue Jin, Xiaojin Shen, Xiaosha Chen, Xiaowen Sun, Xiaoxiang Wang, Xinnan Song, Xinyi Zhou, Xianzu Wang, Xinxia Shan, Y. K. Li, Y. Q. Wang, Y. X. Wei, Yang Zhang, Yanhong Xu, Yao Li, Yao Zhao, Yaofeng Sun, Yaohui Wang, Yi Yu, Yichao Zhang, Yifan Shi, Yiliang Xiong, Ying He, Yishi Piao, Yisong Wang, Yixuan Tan, Yiyang Ma, Yiyuan Liu, Yongqiang Guo, Yuan Ou, Yuduan Wang, Yue Gong, Yuheng Zou, Yujia He, Yunfan Xiong, Yuxiang Luo, Yuxiang You, Yuxuan Liu, Yuyang Zhou, Y. X. Zhu, Yanhong Xu, Yanping Huang, Yaohui Li, Yi Zheng, Yuchen Zhu, Yunxian Ma, Ying Tang, Yukun Zha, Yuting Yan, Z. Z. Ren, Zehui Ren, Zhangli Sha, Zhe Fu, Zhean Xu, Zhenda Xie, Zhengyan Zhang, Zhewen Hao, Zhicheng Ma, Zhigang Yan, Zhiyu Wu, Zihui Gu, Zijia Zhu, Zijun Liu, Zilin Li, Ziwei Xie, Ziyang Song, Zizheng Pan, Zhen Huang, Zhipeng Xu, Zhongyu Zhang, and Zhen Zhang. Deepseek-r1: Incentivizing reasoning capability in llms via reinforcement learning, 2025. URL <https://arxiv.org/abs/2501.12948>.

Angela Fan, Mike Lewis, and Yann Dauphin. Hierarchical neural story generation. *arXiv preprint arXiv:1805.04833*, 2018.

Kanishk Gandhi, Ayush K Chakravarthy, Anikait Singh, Nathan Lile, and Noah Goodman. Cognitive behaviors that enable self-improving reasoners, or, four habits of highly effective STars. In *Second Conference on Language Modeling*, 2025. URL <https://openreview.net/forum?id=QGJ9ttXLTy>.

Aaron Grattafiori, Abhimanyu Dubey, Abhinav Jauhri, Abhinav Pandey, Abhishek Kadian, Ahmad Al-Dahle, Aiesha Letman, Akhil Mathur, Alan Schelten, Alex Vaughan, Amy Yang, Angela Fan, Anirudh Goyal, Anthony Hartshorn, Aobo Yang, Archi Mitra, Archie Sravankumar, Artem Korenev, Arthur Hinsvark, Arun Rao, Aston Zhang, Aurelien Rodriguez, Austen Gregerson, Ava Spataru, Baptiste Roziere, Bethany Biron, Bin Tang, Bobbie Chern, Charlotte Caucheteux, Chaya Nayak, Chloe Bi, Chris Marra, Chris McConnell, Christian Keller, Christophe Touret, Chunyang Wu, Corinne Wong, Cristian Canton Ferrer, Cyrus Nikolaidis, Damien Allonsius, Daniel Song, Danielle Pintz, Danny Livshits, Danny Wyatt, David Esiobu, Dhruv Choudhary, Dhruv Mahajan, Diego Garcia-Olano, Diego Perino, Dieuwke Hupkes, Egor Lakomkin, Ehab AlBadawy, Elina Lobanova, Emily Dinan, Eric Michael Smith, Filip Radenovic, Francisco Guzmán, Frank Zhang, Gabriel Synnaeve, Gabrielle Lee, Georgia Lewis Anderson, Govind That-tai, Graeme Nail, Gregoire Mialon, Guan Pang, Guillem Cucurell, Hailey Nguyen, Hannah Korevaar, Hu Xu, Hugo Touvron, Iliyan Zarov, Imanol Arrieta Ibarra, Isabel Kloumann, Ishan Misra, Ivan Evtimov, Jack Zhang, Jade Copet, Jaewon Lee, Jan Geffert, Jana Vranes, Jason Park, Jay Mahaedokar, Jeet Shah, Jelmer van der Linde, Jennifer Billock, Jenny Hong, Jenya Lee, Jeremy Fu, Jianfeng Chi, Jianyu Huang, Jiawen Liu, Jie Wang, Jiecao Yu, Joanna Bitton, Joe Spisak, Jong-soo Park, Joseph Rocca, Joshua Johnstun, Joshua Saxe, Junteng Jia, Kalyan Vasudevan Alwala, Karthik Prasad, Kartikeya Upasani, Kate Plawiak, Ke Li, Kenneth Heafield, Kevin Stone, Khalid El-Arini, Krithika Iyer, Kshitiz Malik, Kuenley Chiu, Kunal Bhalla, Kushal Lakhotia, Lauren Rantala-Yearly, Laurens van der Maaten, Lawrence Chen, Liang Tan, Liz Jenkins, Louis Martin, Lovish Madaan, Lubo Malo, Lukas Blecher, Lukas Landzaat, Luke de Oliveira, Madeline Muzzi, Mahesh Pasupuleti, Mannat Singh, Manohar Paluri, Marcin Kardas, Maria Tsimpoukelli, Mathew Oldham, Mathieu Rita, Maya Pavlova, Melanie Kambadur, Mike Lewis, Min Si, Mitesh Kumar Singh, Mona Hassan, Naman Goyal, Narjes Torabi, Nikolay Bashlykov, Nikolay Bogoychev, Niladri Chatterji, Ning Zhang, Olivier Duchenne, Onur Çelebi, Patrick Alrassy, Pengchuan Zhang, Pengwei Li, Petar Vasic, Peter Weng, Prajjwal Bhargava, Pratik Dubal, Praveen Krishnan, Punit Singh Koura, Puxin Xu, Qing He, Qingxiao Dong, Ragavan Srinivasan, Raj Ganapathy, Ramon Calderer, Ricardo Silveira Cabral, Robert Stojnic, Roberta Raileanu, Rohan Maheswari, Ro-

hit Girdhar, Rohit Patel, Romain Sauvestre, Ronnie Polidoro, Roshan Sumbaly, Ross Taylor, Ruan Silva, Rui Hou, Rui Wang, Saghar Hosseini, Sahana Chennabasappa, Sanjay Singh, Sean Bell, Seohyun Sonia Kim, Sergey Edunov, Shaoliang Nie, Sharan Narang, Sharath Raparthy, Sheng Shen, Shengye Wan, Shruti Bhosale, Shun Zhang, Simon Vandenhende, Soumya Batra, Spencer Whitman, Sten Sootla, Stephane Collot, Suchin Gururangan, Sydney Borodinsky, Tamar Herman, Tara Fowler, Tarek Sheasha, Thomas Georgiou, Thomas Scialom, Tobias Speckbacher, Todor Mihaylov, Tong Xiao, Ujjwal Karn, Vedanuj Goswami, Vibhor Gupta, Vignesh Ramanathan, Viktor Kerkez, Vincent Gonguet, Virginie Do, Vish Vogeti, Vitor Albiero, Vladan Petrovic, Weiwei Chu, Wenhan Xiong, Wenyin Fu, Whitney Meers, Xavier Martinet, Xiaodong Wang, Xiaofang Wang, Xiaoqing Ellen Tan, Xide Xia, Xinfeng Xie, Xuchao Jia, Xuewei Wang, Yaelle Goldschlag, Yashesh Gaur, Yasmine Babaei, Yi Wen, Yiwen Song, Yuchen Zhang, Yue Li, Yuning Mao, Zacharie Delpierre Coudert, Zheng Yan, Zhengxing Chen, Zoe Papakipos, Aaditya Singh, Aayushi Srivastava, Abha Jain, Adam Kelsey, Adam Shajnfeld, Adithya Gangidi, Adolf Victoria, Ahuva Goldstand, Ajay Menon, Ajay Sharma, Alex Boesenber, Alexei Baevski, Allie Feinstein, Amanda Kallet, Amit Sangani, Amos Teo, Anam Yunus, Andrei Lupu, Andres Alvarado, Andrew Caples, Andrew Gu, Andrew Ho, Andrew Poulton, Andrew Ryan, Ankit Ramchandani, Annie Dong, Annie Franco, Anuj Goyal, Aparajita Saraf, Arkabandhu Chowdhury, Ashley Gabriel, Ashwin Bharambe, Assaf Eisenman, Azadeh Yazdan, Beau James, Ben Maurer, Benjamin Leonhardi, Bernie Huang, Beth Loyd, Beto De Paola, Bhargavi Paranjape, Bing Liu, Bo Wu, Boyu Ni, Braden Hancock, Bram Wasti, Brandon Spence, Brani Stojkovic, Brian Gamido, Britt Montalvo, Carl Parker, Carly Burton, Catalina Mejia, Ce Liu, Changhan Wang, Changkyu Kim, Chao Zhou, Chester Hu, Ching-Hsiang Chu, Chris Cai, Chris Tindal, Christoph Feichtenhofer, Cynthia Gao, Damon Civin, Dana Beaty, Daniel Kreymer, Daniel Li, David Adkins, David Xu, Davide Testuggine, Delia David, Devi Parikh, Diana Liskovich, Didem Foss, Dingkang Wang, Duc Le, Dustin Holland, Edward Dowling, Eissa Jamil, Elaine Montgomery, Eleonora Presani, Emily Hahn, Emily Wood, Eric-Tuan Le, Erik Brinkman, Esteban Arcaute, Evan Dunbar, Evan Smothers, Fei Sun, Felix Kreuk, Feng Tian, Filippos Kokkinos, Firat Ozgenel, Francesco Caggioni, Frank Kanayet, Frank Seide, Gabriela Medina Florez, Gabriella Schwarz, Gada Badeer, Georgia Swee, Gil Halpern, Grant Herman, Grigory Sizov, Guangyi, Zhang, Guna Lakshminarayanan, Hakan Inan, Hamid Shojaanazeri, Han Zou, Hannah Wang, Hanwen Zha, Haroun Habeeb, Harrison Rudolph, Helen Suk, Henry Aspegren, Hunter Goldman, Hongyuan Zhan, Ibrahim Damlaj, Igor Molybog, Igor Tufanov, Ilias Leontiadis, Irina-Elena Veliche, Itai Gat, Jake Weissman, James Geboski, James Kohli, Janice Lam, Japhet Asher, Jean-Baptiste Gaya, Jeff Marcus, Jeff Tang, Jennifer Chan, Jenny Zhen, Jeremy Reizenstein, Jeremy Teboul, Jessica Zhong, Jian Jin, Jingyi Yang, Joe Cummings, Jon Carvill, Jon Shepard, Jonathan McPhie, Jonathan Torres, Josh Ginsburg, Junjie Wang, Kai Wu, Kam Hou U, Karan Saxena, Kartikay Khandelwal, Katayoun Zand, Kathy Matosich, Kaushik Veeraraghavan, Kelly Michelena, Keqian Li, Kiran Jagadeesh, Kun Huang, Kunal Chawla, Kyle Huang, Lailin Chen, Lakshya Garg, Lavender A, Leandro Silva, Lee Bell, Lei Zhang, Liangpeng Guo, Licheng Yu, Liron Moshkovich, Luca Wehrstedt, Madian Khabsa, Manav Avalani, Manish Bhatt, Martynas Mankus, Matan Hasson, Matthew Lennie, Matthias Reso, Maxim Groshev, Maxim Naumov, Maya Lathi, Meghan Keneally, Miao Liu, Michael L. Seltzer, Michal Valko, Michelle Restrepo, Mihir Patel, Mik Vyatskov, Mikayel Samvelyan, Mike Clark, Mike Macey, Mike Wang, Miquel Jubert Hermoso, Mo Metanat, Mohammad Rastegari, Munish Bansal, Nandhini Santhanam, Natascha Parks, Natasha White, Navyata Bawa, Nayan Singhal, Nick Egebo, Nicolas Usunier, Nikhil Mehta, Nikolay Pavlovich Laptev, Ning Dong, Norman Cheng, Oleg Chernoguz, Olivia Hart, Omkar Salpekar, Ozlem Kalinli, Parkin Kent, Parth Parekh, Paul Saab, Pavan Balaji, Pedro Rittner, Philip Bontrager, Pierre Roux, Piotr Dollar, Polina Zvyagina, Prashant Ratanchandani, Pritish Yuvraj, Qian Liang, Rachad Alao, Rachel Rodriguez, Rafi Ayub, Raghatham Murthy, Raghu Nayani, Rahul Mitra, Rangaprabhu Parthasarathy, Raymond Li, Rebekkah Hogan, Robin Battey, Rocky Wang, Russ Howes, Ruty Rinott, Sachin Mehta, Sachin Siby, Sai Jayesh Bondu, Samyak Datta, Sara Chugh, Sara Hunt, Sargun Dhillon, Sasha Sidorov, Satadru Pan, Saurabh Mahajan, Saurabh Verma, Seiji Yamamoto, Sharadh Ramaswamy, Shaun Lindsay, Shaun Lindsay, Sheng Feng, Shenghao Lin, Shengxin Cindy Zha, Shishir Patil, Shiva Shankar, Shuqiang Zhang, Shuqiang Zhang, Sinong Wang, Sneha Agarwal, Soji Sajuyigbe, Soumith Chintala, Stephanie Max, Stephen Chen, Steve Kehoe, Steve Satterfield, Sudarshan Govindaprasad, Sumit Gupta, Summer Deng, Sungmin Cho, Sunny Virk, Suraj Subramanian, Sy Choudhury, Sydney Goldman, Tal Remez, Tamar Glaser, Tamara Best, Thilo Koehler, Thomas Robinson, Tianhe Li, Tianjun Zhang, Tim Matthews, Timothy Chou, Tzook Shaked, Varun Vontimitta, Victoria Ajayi, Victoria Montanez, Vijai Mohan, Vinay Satish Ku-

mar, Vishal Mangla, Vlad Ionescu, Vlad Poenaru, Vlad Tiberiu Mihailescu, Vladimir Ivanov, Wei Li, Wencheng Wang, Wenwen Jiang, Wes Bouaziz, Will Constable, Xiaocheng Tang, Xaojian Wu, Xiaolan Wang, Xilun Wu, Xinbo Gao, Yaniv Kleinman, Yanjun Chen, Ye Hu, Ye Jia, Ye Qi, Yenda Li, Yilin Zhang, Ying Zhang, Yossi Adi, Youngjin Nam, Yu, Wang, Yu Zhao, Yuchen Hao, Yundi Qian, Yunlu Li, Yuzi He, Zach Rait, Zachary DeVito, Zef Rosnbrick, Zhao-duo Wen, Zhenyu Yang, Zhiwei Zhao, and Zhiyu Ma. The llama 3 herd of models, 2024. URL <https://arxiv.org/abs/2407.21783>.

Etash Guha, Ryan Marten, Sedrick Keh, Negin Raoof, Georgios Smyrnis, Hritik Bansal, Marianna Nezhurina, Jean Mercat, Trung Vu, Zayne Sprague, Ashima Suvarna, Benjamin Feuer, Liangyu Chen, Zaid Khan, Eric Frankel, Sachin Grover, Caroline Choi, Niklas Muennighoff, Shiye Su, Wanja Zhao, John Yang, Shreyas Pimpalaonkar, Kartik Sharma, Charlie Cheng-Jie Ji, Yichuan Deng, Sarah Pratt, Vivek Ramanujan, Jon Saad-Falcon, Jeffrey Li, Achal Dave, Alon Albalak, Kushal Arora, Blake Wulfe, Chinmay Hegde, Greg Durrett, Sewoong Oh, Mohit Bansal, Saadia Gabriel, Aditya Grover, Kai-Wei Chang, Vaishaal Shankar, Aaron Gokaslan, Mike A. Merrill, Tatsunori Hashimoto, Yejin Choi, Jenia Jitsev, Reinhard Heckel, Maheswaran Sathiamoorthy, Alexandros G. Dimakis, and Ludwig Schmidt. Openthoughts: Data recipes for reasoning models, 2025. URL <https://arxiv.org/abs/2506.04178>.

Ari Holtzman, Jan Buys, Li Du, Maxwell Forbes, and Yejin Choi. The curious case of neural text degeneration. In *International Conference on Learning Representations*, 2020. URL <https://openreview.net/forum?id=rygGQyrFvH>.

Edward S. Hu, Kwangjun Ahn, Qinghua Liu, Haoran Xu, Manan Tomar, Ada Langford, Dinesh Jayaraman, Alex Lamb, and John Langford. The belief state transformer. In *The Thirteenth International Conference on Learning Representations*, 2025. URL <https://openreview.net/forum?id=ThRMTGpvo>.

Aaron Jaech, Adam Kalai, Adam Lerer, Adam Richardson, Ahmed El-Kishky, Aiden Low, Alec Helyar, Aleksander Madry, Alex Beutel, Alex Carney, et al. Openai o1 system card. *arXiv preprint arXiv:2412.16720*, 2024.

Nitish Shirish Keskar, Bryan McCann, Lav R Varshney, Caiming Xiong, and Richard Socher. Ctrl: A conditional transformer language model for controllable generation. *arXiv preprint arXiv:1909.05858*, 2019.

Dacheng Li, Shiyi Cao, Tyler Griggs, Shu Liu, Xiangxi Mo, Eric Tang, Sumanth Hegde, Kourosh Hakhamaneshi, Shishir G. Patil, Matei Zaharia, Joseph E. Gonzalez, and Ion Stoica. Llms can easily learn to reason from demonstrations structure, not content, is what matters!, 2025. URL <https://arxiv.org/abs/2502.07374>.

Huayang Li, Tian Lan, Zihao Fu, Deng Cai, Lemao Liu, Nigel Collier, Taro Watanabe, and Yixuan Su. Repetition in repetition out: Towards understanding neural text degeneration from the data perspective. In *Thirty-seventh Conference on Neural Information Processing Systems*, 2023. URL <https://openreview.net/forum?id=WjgCRrOgip>.

Rajeev Motwani and Prabhakar Raghavan. Randomized algorithms. *ACM Computing Surveys (CSUR)*, 28(1):33–37, 1996.

David Rein, Betty Li Hou, Asa Cooper Stickland, Jackson Petty, Richard Yuanzhe Pang, Julien Dirani, Julian Michael, and Samuel R. Bowman. GPQA: A graduate-level google-proof q&a benchmark. In *First Conference on Language Modeling*, 2024. URL <https://openreview.net/forum?id=Ti67584b98>.

Shai Shalev-Shwartz, Ohad Shamir, and Shaked Shammah. Failures of gradient-based deep learning. In *International Conference on Machine Learning*, pp. 3067–3075. PMLR, 2017.

Yixuan Su and Nigel Collier. Contrastive search is what you need for neural text generation. *Transactions on Machine Learning Research*, 2023. ISSN 2835-8856. URL <https://openreview.net/forum?id=GbkWw3jwL9>.

- Yixuan Su, Tian Lan, Yan Wang, Dani Yogatama, Lingpeng Kong, and Nigel Collier. A contrastive framework for neural text generation. In Alice H. Oh, Alekh Agarwal, Danielle Belgrave, and Kyunghyun Cho (eds.), *Advances in Neural Information Processing Systems*, 2022. URL <https://openreview.net/forum?id=V88BafmH9Pj>.
- Qwen Team. Qwq-32b: Embracing the power of reinforcement learning, March 2025. URL <https://qwenlm.github.io/blog/qwq-32b/>.
- Salil P Vadhan et al. Pseudorandomness. *Foundations and Trends® in Theoretical Computer Science*, 7(1–3):1–336, 2012.
- Sean Welleck, Ilia Kulikov, Stephen Roller, Emily Dinan, Kyunghyun Cho, and Jason Weston. Neural text generation with unlikelihood training. In *International Conference on Learning Representations*, 2020. URL <https://openreview.net/forum?id=SJeYe0NtvH>.
- Jin Xu, Xiaojiang Liu, Jianhao Yan, Deng Cai, Huayang Li, and Jian Li. Learning to break the loop: Analyzing and mitigating repetitions for neural text generation. *Advances in Neural Information Processing Systems*, 35:3082–3095, 2022.
- An Yang, Baosong Yang, Binyuan Hui, Bo Zheng, Bowen Yu, Chang Zhou, Chengpeng Li, Chengyuan Li, Dayiheng Liu, Fei Huang, Guanting Dong, Haoran Wei, Huan Lin, Jialong Tang, Jialin Wang, Jian Yang, Jianhong Tu, Jianwei Zhang, Jianxin Ma, Jin Xu, Jingren Zhou, Jinze Bai, Jinzheng He, Junyang Lin, Kai Dang, Keming Lu, Keqin Chen, Kexin Yang, Mei Li, Mingfeng Xue, Na Ni, Pei Zhang, Peng Wang, Ru Peng, Rui Men, Ruize Gao, Runji Lin, Shijie Wang, Shuai Bai, Sinan Tan, Tianhang Zhu, Tianhao Li, Tianyu Liu, Wenbin Ge, Xiaodong Deng, Xiaohuan Zhou, Xingzhang Ren, Xinyu Zhang, Xipin Wei, Xuancheng Ren, Yang Fan, Yang Yao, Yichang Zhang, Yu Wan, Yunfei Chu, Yuqiong Liu, Zeyu Cui, Zhenru Zhang, and Zhihao Fan. Qwen2 technical report. *arXiv preprint arXiv:2407.10671*, 2024a.
- An Yang, Beichen Zhang, Binyuan Hui, Bofei Gao, Bowen Yu, Chengpeng Li, Dayiheng Liu, Jianhong Tu, Jingren Zhou, Junyang Lin, Keming Lu, Mingfeng Xue, Runji Lin, Tianyu Liu, Xingzhang Ren, and Zhenru Zhang. Qwen2.5-math technical report: Toward mathematical expert model via self-improvement, 2024b.

## A ADDITIONAL EXPERIMENTAL DETAILS ON SECTION 2

**Evaluation details.** We used the Eureka ML Insights Framework (Balachandran et al., 2024; 2025) to conduct the evaluations on all models. For the inference parameters, we kept the default `top_k` and `top_p` for each model, taken from its HuggingFace repository. We do not use any repetition penalty as we focus on the role of temperature. We ran all reasoning models with a 30K `max_tokens` budget and all instruct models, we set it based on the max allowed number of tokens for each model (14k for Phi-4, 3k for Qwen2.5-Math-1.5B-Instruct, 30k for Llama-3.1-8B-Instruct and Qwen2.5-1.5B-Instruct).

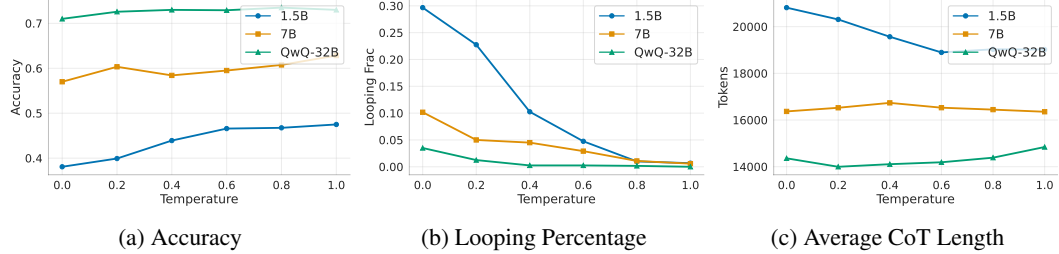


Figure 6: Openthinker metrics as a function of temperature.

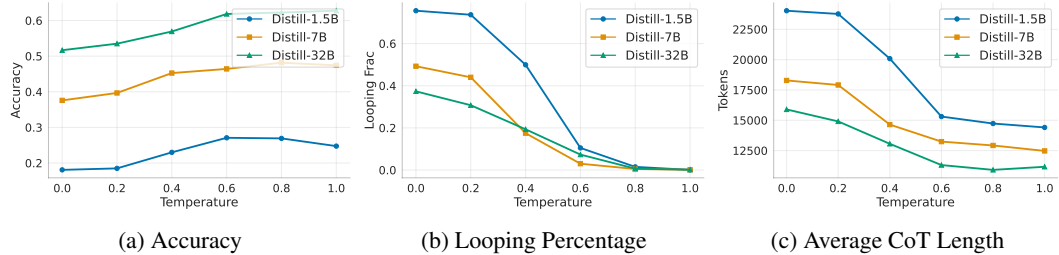


Figure 7: Qwen metrics as a function of temperature.

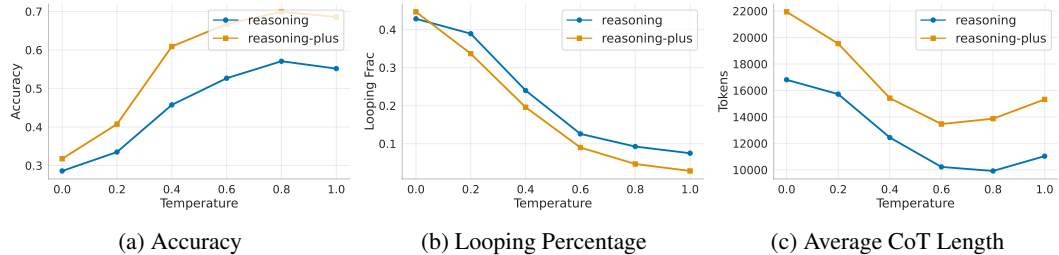


Figure 8: Phi-4 metrics as a function of temperature

**Phi-4 reasoning models on hard and easy problems.** The Phi-4 reasoning family of models was the only exception to the observation that hard problems induce more looping than easy ones. As we can see in Figure 10, both phi-4-reasoning and phi-4-reasoning-plus consistently exhibit more looping in easier problems than in hard ones. By manually inspecting its responses, we realized that it very often demonstrates a peculiar form of looping; it finds the answer during the CoT, then proceeds to present it, and then it gets stuck indefinitely repeating things like “We’ll produce answer in plain text.” This is one of the main ways in which it loops, which means that for easy problems, it will reach the solution more frequently and, thus, get stuck in this situation more often than in harder problems. Note also that another key way in which phi-4-reasoning models differ from the other models we tested is that it has been fine-tuned on OpenAI o4-mini data (Abdin et al., 2025), as opposed to DeepSeek-R1 or Qwen. Nevertheless, this is only a preliminary attempt at explaining this discrepancy and a more thorough study of the exact underlying factors would make a great direction for future research.

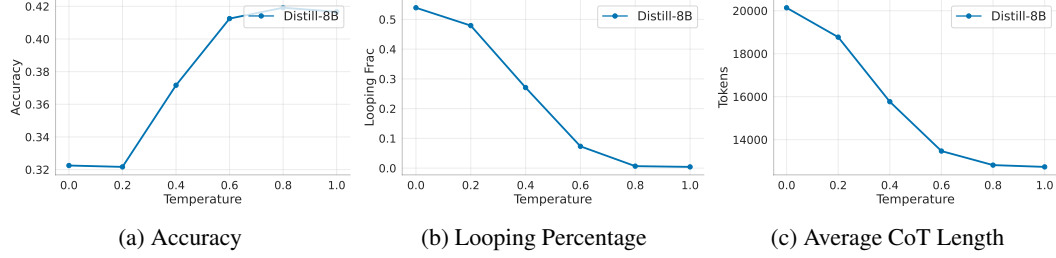


Figure 9: Llama metrics as a function of temperature.

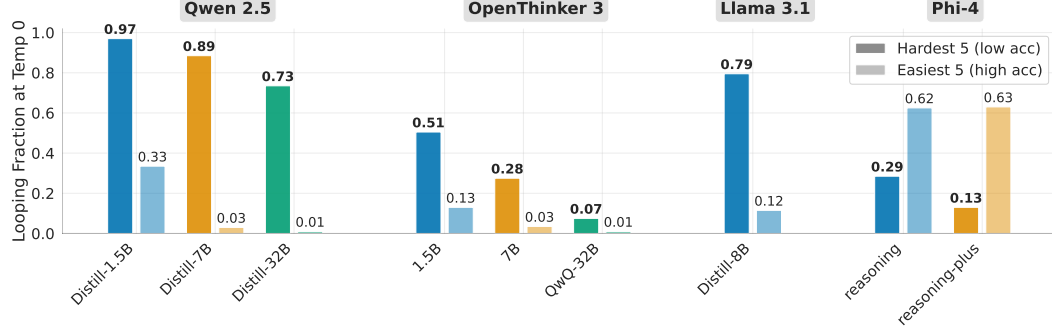


Figure 10: **Looping with greedy decoding for a hard-easy split of AIME problems.** For each model, we use *accuracies at temperature 0.8* to create a split of the 5 easiest problems and 5 hardest problems. Then we evaluate the *looping percentage at temperature 0* separately on these two sets of problems. The bars on the left show the looping percentage on hard problems and bars on the right show the percentage on easy problems. We can see that for all model families except Phi-4, models looping significantly more in hard problems than in easy ones.

### A.1 ABLATIONS ON THE $(n, k)$ DEFINITION OF LOOPING

In this section we ablate the  $(n, k)$  definition of looping, each time keeping either  $n$  or  $k$  fixed and varying the other parameter. The results for different parameter settings are shown in Table 1. Note that looping percentages do not have any significant differences and the relative ordering of all models remains the same in all cases. This is not very surprising, considering our original definition of  $n = 30, k = 20$  is already very strict; to consider a text as containing looping it must contain a 30-gram at least 20 times.

Model	(20,20)	(30,20)	(30,30)	(30,60)	(40,20)
R1-Distill-Qwen-1.5B	0.76	0.76	0.75	0.72	0.75
R1-Distill-Qwen-7B	0.51	0.49	0.48	0.41	0.49
R1-Distill-Qwen-32B	0.40	0.37	0.33	0.22	0.36
OpenThinker3-1.5B	0.33	0.30	0.28	0.27	0.29
OpenThinker3-7B	0.12	0.10	0.09	0.09	0.09
QwQ-32B	0.04	0.04	0.03	0.03	0.03
R1-Distill-Llama-8B	0.56	0.54	0.51	0.41	0.53
Phi-4-reasoning	0.46	0.43	0.42	0.41	0.42
Phi-4-reasoning-plus	0.49	0.45	0.44	0.42	0.44

Table 1: Looping percentages at temperature 0 for different  $(n, k)$  combinations

### A.2 LOOPING PERCENTAGES ON GPQA

To investigate whether our observations from the AIME dataset transfer to different domains, we ran an ablation with Openthinker3 and Qwen2.5 models on the GPQA Diamond dataset (Rein et al.,

2024), which contains a set of 198 highly challenging questions from biology, physics, and chemistry. For each (model, problem, temperature) tuple we generate 4 responses , for a total of  $\approx 800$  responses at each (model, temperature). We evaluate on temperatures 0.0, 0.4, 0.8. We see that our main observations also hold here: lower-capacity models loop more and student models loop significantly more than teacher.

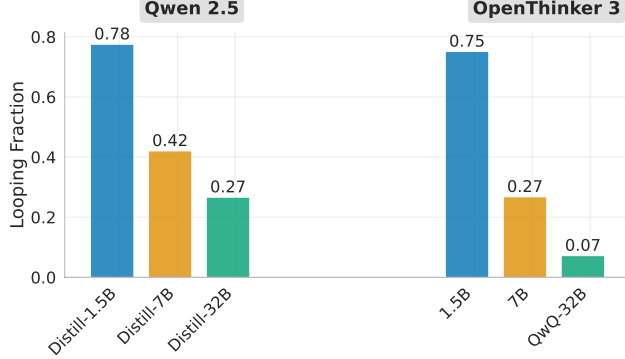


Figure 11: Looping with greedy decoding on GPQA.

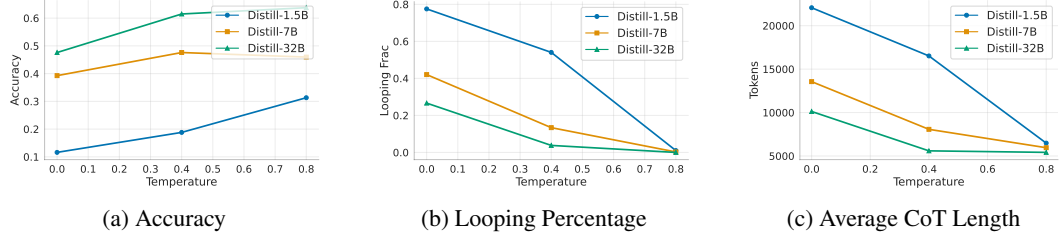


Figure 12: Qwen metrics on GPQA as a function of temperature.

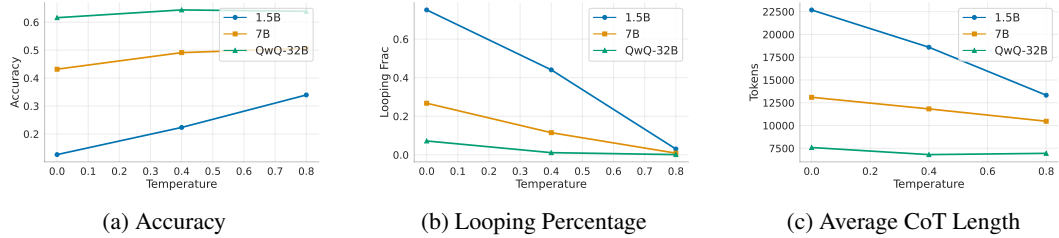


Figure 13: Openthinker metrics on GPQA as a function of temperature.

## B ANOTHER EXAMPLE TRACE

**Example 2.** Here, we prompt Openthinker-3 1.5B to solve Problem I-5 from AIME 2025, with greedy decoding:

There are  $8! = 40320$  eight-digit positive integers that use each of the digits 1, 2, 3, 4, 5, 6, 7, 8 exactly once. Let  $N$  be the number of these integers that are divisible by 22. Find the difference between  $N$  and 2025.

The model starts well. It recalls that being divisible by 22 means being divisible by both 2 and 11, notes that the last digit must be even, and sets up the standard 11-divisibility condition in terms of the sums of digits in odd and even positions.

Okay, so I need to find the number of eight-digit numbers using each of the digits 1 through 8 exactly once that are divisible by 22. . . .

First, a number divisible by 22 must be divisible by both 2 and 11. Since 22 is 2 times 11, and 2 and 11 are coprime, the number has to satisfy the divisibility rules for both 2 and 11.

Starting with divisibility by 2: For a number to be divisible by 2, its last digit must be even. So the last digit has to be one of 2, 4, 6, or 8. That gives me a starting point.

Now, divisibility by 11: The rule for 11 is that the difference between the sum of the digits in the odd positions and the sum of the digits in the even positions must be a multiple of 11 (including zero). Since we're dealing with an eight-digit number, the positions are 1 to 8. So, the first, third, fifth, seventh digits are the odd positions, and the second, fourth, sixth, eighth digits are the even positions.

Let me formalize this. Let the number be D1 D2 D3 D4 D5 D6 D7 D8. Then, the sum of the odd positions is  $S_{\text{odd}} = D_1 + D_3 + D_5 + D_7$ , and the sum of the even positions is  $S_{\text{even}} = D_2 + D_4 + D_6 + D_8$ . The difference  $(S_{\text{odd}} - S_{\text{even}})$  must be divisible by 11.

From here it makes correct algebraic progress on the 11-rule: it rewrites the condition in terms of  $S_{\text{odd}}$  alone, reduces modulo 11, and finds that  $S_{\text{odd}} \equiv 7 \pmod{11}$ . It then uses the fact that  $S_{\text{odd}}$  is the sum of four distinct digits from  $\{1, \dots, 8\}$  and correctly narrows down to the only feasible value.

Since all digits from 1 to 8 are used exactly once, the total sum of all digits is  $1 + 2 + 3 + 4 + 5 + 6 + 7 + 8 = 36$ . Therefore,  $S_{\text{odd}} + S_{\text{even}} = 36$ .

So, the difference  $(S_{\text{odd}} - S_{\text{even}})$  must be a multiple of 11. Let me denote  $D = S_{\text{odd}} - S_{\text{even}}$ . Then,  $D = S_{\text{odd}} - (36 - S_{\text{odd}}) = 2 * S_{\text{odd}} - 36$ . Therefore,  $2 * S_{\text{odd}} - 36$  must be divisible by 11.

So,  $2 * S_{\text{odd}} \equiv 36 \pmod{11}$ . Let me compute  $36 \pmod{11}$ .  $11 * 3 = 33$ , so  $36 - 33 = 3$ , so  $36 \equiv 3 \pmod{11}$ . Therefore,  $2 * S_{\text{odd}} \equiv 3 \pmod{11}$ .

To solve for  $S_{\text{odd}}$ , we can multiply both sides by the modular inverse of 2 ( $\pmod{11}$ ). The inverse of 2 ( $\pmod{11}$ ) is 6 because  $2 * 6 = 12 \equiv 1 \pmod{11}$ . Therefore, multiplying both sides by 6 gives  $S_{\text{odd}} \equiv 3 * 6 \pmod{11}$ , which is 18 ( $\pmod{11}$ ), which is 7 ( $\pmod{11}$ ).

Therefore,  $S_{\text{odd}} \equiv 7 \pmod{11}$ . Since  $S_{\text{odd}}$  is the sum of four distinct digits from 1 – 8, let's find all possible values of  $S_{\text{odd}}$  that are congruent to 7 ( $\pmod{11}$ ).

First, the possible range of  $S_{\text{odd}}$ . The minimal possible sum of four distinct digits is  $1 + 2 + 3 + 4 = 10$ , and the maximum is  $5 + 6 + 7 + 8 = 26$ . So  $S_{\text{odd}}$  can be between 10 and 26.

We need  $S_{\text{odd}} \equiv 7 \pmod{11}$ . Let's see which numbers between 10 and 26 are congruent to 7 ( $\pmod{11}$ ).

7 ( $\pmod{11}$ ) is 7,  $7 + 11 = 18$ ,  $18 + 11 = 29$ , but 29 is beyond 26. So the only possible value is 18. Wait, 7 ( $\pmod{11}$ ) is 7, but 7 is less than 10, so the next one is 18. 18 is within 10 – 26, so  $S_{\text{odd}}$  must be 18.

Wait, but 7 ( $\pmod{11}$ ) is 7, but since  $S_{\text{odd}}$  must be at least 10, the next possible is 18. So  $S_{\text{odd}}$  must equal 18.

Therefore, the sum of the digits in the odd positions must be 18, and the sum of the even positions will then be  $36 - 18 = 18$  as well.

At this point the model makes its first key mistake. When it fixes the last digit  $E$  to be even and looks at the remaining 7 digits, it continues to insist that the four digits in the odd positions must sum to 18 and the three digits in the remaining even positions must also sum to 18, as if the last digit had disappeared.

Additionally, the last digit (position 8) must be even (2, 4, 6, 8) to satisfy divisibility by 2.

Therefore, we can approach this problem in steps:

1. First, choose the last digit (position 8) to be even. There are 4 choices (2, 4, 6, 8).

2. Then, partition the remaining 7 digits into two groups: the first, third, fifth, seventh positions (four digits) and the second, fourth, sixth positions (three digits). Wait, no, actually, the remaining digits after choosing the last digit are 7 digits, but the even positions (positions 2, 4, 6, 8) need to have three digits (since position 8 is already chosen). Wait, let me clarify:

Wait, actually, the even positions are positions 2, 4, 6, 8. Since position 8 is already fixed as an even digit, the remaining even positions (positions 2, 4, 6) must be filled with three digits from the remaining seven digits (since one even digit is already used in position 8). The odd positions (positions 1, 3, 5, 7) must be filled with the remaining four digits.

Therefore, the total digits to assign are 7 digits (since one even digit is used in position 8). These 7 digits must be split into two groups: four digits for the odd positions (positions 1, 3, 5, 7) and three digits for the even positions (positions 2, 4, 6). The sum of the four digits in the odd positions must be 18, and the sum of the three digits in the even positions must be 18 (since total sum is 36, so  $36 - 18 = 18$ ).

This leads to a contradiction ( $E$  would have to be 0), and the model notices that something is wrong.

Therefore, the problem reduces to:

...  
First, let me note that the last digit is fixed as an even digit (2, 4, 6, 8). Let's denote the last digit as  $E$ .

...  
We need to choose 4 digits from these 7 to be in the odd positions (positions 1,3,5,7) such that their sum is 18, and the remaining 3 digits will be in the even positions (positions 2,4,6) with sum 18.  
Therefore, for each  $E$ , we need to compute the number of 4-element subsets of the remaining 7 digits that sum to 18, and then for each such subset, the number of permutations is  $4!$  (for the odd positions) multiplied by  $3!$  (for the even positions).

...  
Wait, let's see. Let me first compute the total sum of the remaining 7 digits when  $E$  is removed. The total sum of all digits is 36, so the remaining sum is  $36 - E$ .

...  
Therefore, the sum of the 3 digits (even positions) is 18, so the sum of the 4 digits (odd positions) is 18.

...  
Therefore, the total sum of the 7 digits (excluding  $E$ ) is  $18 + 18 = 36 - E$ .  
Therefore,  $36 - E$  must equal 36, so that  $36 - E = 36$ ? Wait, that can't be. Wait,  $18 + 18 = 36$ , so  $36 - E$  must equal 36? That would mean  $E = 0$ , but  $E$  is an even digit from 2, 4, 6, 8.

...  
Wait, that's a contradiction. That suggests that my earlier reasoning is wrong.  
Hmm, so where did I go wrong? Let me check again.

However, instead of changing its approach, it falls into a loop: it repeatedly restates the divisibility-by-11 condition, re-derives  $S_{\text{odd}} \equiv 7 \pmod{11}$ , concludes again that  $S_{\text{odd}} = 18$ , and runs back into the same contradiction with  $E$ .

Wait, let me go back.  
We had  $S_{\text{odd}} - S_{\text{even}} \equiv 0 \pmod{11}$ , and  $S_{\text{odd}} + S_{\text{even}} = 36$ .

...  
Therefore,  $S_{\text{odd}} \equiv 7 \pmod{11}$ .

...  
But then, the total of the seven digits (excluding the last digit  $E$ ) must be  $18 + 18 = 36$ , so  $36 - E = 36 \Rightarrow E = 0$ .  
But  $E$  is an even digit from 2,4,6,8.

This is a contradiction.  
[Semantically loops essentially repeating the same mistake 5 more times]

This behavior bears similarity to the temporally correlated errors we saw in our graph reasoning setting: once the model makes a high-level mistake, it keeps returning to the same wrong reasoning whenever it tries to restart. In the graph setting, this corresponded to repeatedly picking the same wrong child at the root, leading to the same leaf, and restarting.

After several rounds of semantic looping, the model makes a new mistake! It now claims that  $S_{\text{odd}} + S_{\text{even}} = 36 - E$  instead of 36, which it had correctly used earlier. Building on this, it mistakenly concludes  $2S_{\text{odd}} \equiv 36 - E \pmod{11}$  (instead of  $2S_{\text{odd}} \equiv 36 \pmod{11}$ , which it correctly found earlier). It follows up with a case analysis over  $E \in \{2, 4, 6, 8\}$ .

Wait,  $S_{\text{odd}} + S_{\text{even}} = 36 - E$ .

...  
Therefore,  $2S_{\text{odd}} \equiv 36 - E \pmod{11}$ .

Ah! So my earlier mistake was not including the  $E$  term.

...  
Therefore, for each  $E$ , possible  $S_{\text{odd}}$  values are:

$E = 2: S_{\text{odd}} = 17$   
 $E = 4: S_{\text{odd}} = 16$   
 $E = 6: S_{\text{odd}} = 15 \text{ or } 26$   
 $E = 8: S_{\text{odd}} = 14 \text{ or } 25$



**Further analysis (first loop).** To probe this behavior further, we truncate the trace at the point where the model first reaches a contradiction (right after it concludes that  $E$  would have to be 0). From this prefix, we let the teacher model (QwQ-32B) continue under greedy decoding and generate 5 continuations to account for non-determinism. In all traces, the teacher immediately identifies the mistake, repairs the reasoning, and eventually reaches the correct answer. We also generate 5 new continuations from the student (OpenThinker-3 1.5B) from the same prefix. This time we see two distinct student traces: both loop 2-3 more times, repeatedly re-deriving the same wrong condition and contradiction, but eventually notice the mistake. Once they exit this first loop, they start a case-by-case analysis in  $E$  and then get stuck again in a loop, similar to the second loop in the above trace.

To get a quantitative sense of how much probability mass the two models place on the progress-making action of correctly escaping the contradiction, we sample 50 continuations of length 1000 tokens from each model at temperatures 0.7 and 1.0 from the same truncated prefix. We then ask GPT-5 to check whether each continuation correctly fixes the mistaken equation and moves on with valid reasoning. At temperature 0.7, GPT-5 marks 19/50 student continuations and 50/50 teacher continuations as successfully escaping the contradiction; at temperature 1.0, these numbers are 21/50 and 48/50, respectively. Thus, the teacher puts much more mass on the correct progress-making action than the student.

Overall, this first loop shows glimpses of the temporally correlated errors mechanism from Section 4: once the student falls into a wrong pattern, it tends to revisit the same mistaken step several times. Here, the gap between the teacher and the student is relatively large, for example in terms of how much probability mass they put on the correct progress-making action. In this sense, the behavior is closer in spirit to our margin variant (where, after pursuing an action once, the teacher shifts more probability to other actions) or to the hardness+correlated-errors variant in Appendix D, where we show that temporally correlated errors can arise even when the teacher distribution puts high mass on the correct progress-making action.

**Second loop.** We also probe the second looping point by truncating the trace right when the model gets stuck in the final infinite loop (at the point after it says “ $7 + 6 + 4 = 17, 7 + 5 + 5 = \text{no}$ ”). From this prefix, we again generate 5 greedy continuations from both the teacher (QwQ-32B) and the student (OpenThinker-3 1.5B). Interestingly, in this case, along with the student, all teacher continuations get stuck in the same loop.

Further, we sample 50 continuations of length 2000 tokens from each model at temperatures 0.7 and 1.0, starting from the same truncated prefix. We then ask GPT-5 whether each continuation makes progress, where we define progress as continuing the enumeration and correctly counting the valid tuples for the  $E = 2$  case. At temperature 0.7, GPT-5 marks 10/50 student continuations and 34/50 teacher continuations as making progress; at temperature 1.0, these numbers are 27/50 and 42/50, respectively. Thus, the teacher still puts more mass on the correct progress-making actions than the student, but the gap is less substantial, especially at temperature 1.

This second loop is interesting because here we see risk-aversion-style looping in both the student and the teacher. There are several possible reasons for why a teacher might also loop.

First, the teacher itself may carry errors in learning from its own training process. Even if it was trained with reinforcement learning, hardness of learning (as discussed in Section 3.3) can still cause it to loop.

Second, note that the teacher did not loop when we started it from the earlier looping point: from that earlier prefix, it was able to identify the mistake and reach the correct answer. In contrast, when we start it from the later point, it is conditioned on a student trace that has already semantically looped several times (repeating the same mistaken reasoning and contradiction). This suggests that error accumulation in the prefix may also play a role: for example, in-context learning from a “confused” history could cause the teacher itself to behave in a more confused, looping way. As we discuss in Section 5, understanding the precise mechanisms by which this kind of error amplification drives loops is an interesting direction for future work.

## C PROOF OF PROPOSITION 1

We restate the proposition below and provide its proof.

**Proposition 1.** Consider the following task: there exist  $n$  sets of contexts  $C_1, \dots, C_n$  which are equi-likely under the training distribution. And there are  $n$  distinct “hard” actions  $a_1, \dots, a_n$ , and an “easy” action  $a_0$ . For every context  $c_i \in C_i$ , the training distribution picks action  $a_i$  with probability  $(1-p)$  and  $a_0$  with probability  $p$ . Now consider a learner that cannot distinguish between the  $n$  hard actions or, in other words, it is constrained to ignore the context when deciding on the best action. Then the maximum log-likelihood solution for such a learner assigns probability  $p$  to the easy action  $a_0$  and probability  $(1-p)/n$  to the hard indistinguishable actions  $a_i, \forall i \in \{1, \dots, n\}$ .

*Proof.* Let  $q_1, \dots, q_n$  be the probabilities that the model assigns to the  $n$  actions, and  $q_0$  be the probability of the easy action. The Cross-Entropy loss for a context  $c_i \in C_i$  with correct action  $a_i$  is

$$\ell_i = -p \log(q_0) - (1-p) \log(q_i).$$

Since all  $n$  contexts are equi-probable, the average Cross Entropy over the dataset will be

$$\begin{aligned} \ell &= \frac{1}{n} \sum_{i=1}^n \ell_i \\ &= -p \log(q_0) - (1-p) \frac{1}{n} \sum_{i=1}^n \log(q_i). \end{aligned}$$

Note that  $\sum_{i=0}^n q_i = 1$  and  $q_i \geq 0$  for all  $i$ , by definition. We can further assume that  $q_i > 0$ , otherwise the loss would be infinite. This is a convex minimization problem under linear constraints, so to find the minimizer it suffices to look at the points satisfying the KKT conditions. In particular,

$$\begin{aligned} \frac{p}{q_0} = \mu &\implies q_0 = \frac{1}{\mu} p \\ \frac{1-p}{n} \frac{1}{q_i} = \mu &\implies q_i = \frac{1}{\mu} (1-p)/n \text{ for } i = 1, \dots, n, \end{aligned}$$

for some  $\mu \in \mathbb{R}$ . Using the equality constraint, we conclude that  $\mu = 1$  and  $q_0 = p, q_i = (1-p)/n$  for  $i = 1, \dots, n$  is the unique minimizer of the problem, as desired.  $\square$

## D LOOPING VIA A COMBINATION OF HARDNESS + CORRELATED ERRORS

In Section 3, we saw how hardness of learning can cause looping and in Section 4 we saw how an inductive bias for correlated errors can lead to looping. In this section, we present yet another variant showing how both hardness and correlated errors can act together and cause looping. In particular, we show that Transformers can have temporally correlated errors even when the teacher puts substantial mass on the correct progress-making action, as opposed to the random uniform distribution we considered in Section 4.

**Setup.** We use the same star graph and random walk as in Section 4, with a minor modification at the root. Instead of choosing a child uniformly at random at the root, the training distribution now goes to the correct child (leading to goal) with probability 0.5 and with probability 0.5, chooses one of the other children uniformly at random. We train a Transformer on traces drawn from this process for the  $G(5, 5)$  graph; training and test details match the previous synthetic experiments.

For our looping metric, like in Section 4, we use the maximum count of times that a root child is visited and average over all 500 generated traces. The results for  $G(5, 5)$  are shown in Figure 14. We observe non-trivial amount of looping at temperature 0, but the looping is not as strong as the walk that picked uniformly random children at the root. Note that a perfect learner would directly go to the correct child with greedy decoding, which would correspond to a looping count of 1.

**Interpretation.** Similar to Section 3, the model initially finds it hard to distinguish between the actions available at the root. This hardness of learning pushes it toward placing roughly equal mass on all root children, even though the training distribution gives probability 0.5 to the correct child

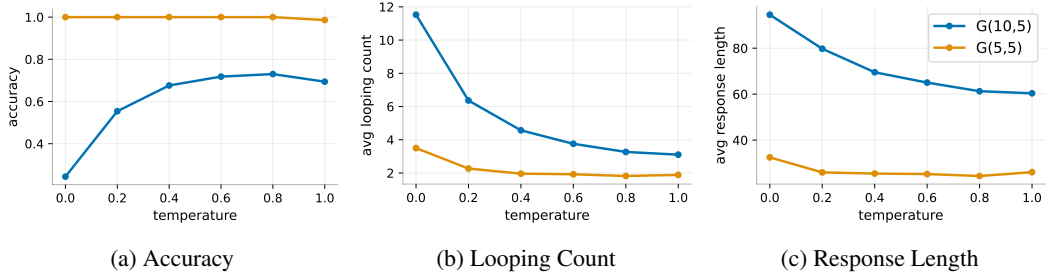


Figure 14: **Looping from combined hardness and temporally correlated errors.** We work in a variant of the correlated-errors setting from Section 4. For  $G(5,5)$  (orange), the setup is the same as in the previous section except for a minor change at the root: instead of choosing a child uniformly, the training distribution now goes to the correct child with probability 0.5 and to each of the four wrong children with probability  $0.5/4$ . For  $G(10,5)$  (blue), the root distribution again puts 0.5 on the correct child but spreads the remaining 0.5 over only four of the nine wrong children. On  $G(5,5)$ , looping is still present but relatively weak and accuracy is near perfect. On  $G(10,5)$ , looping is much stronger at low temperature and response lengths are substantially longer, especially under greedy decoding. Overall, this shows that looping similar to Section 4 can occur even when the training distribution places significant mass on the correct progress-making action.

and  $0.5/4$  to each of the four incorrect children. Once this happens, the situation seems similar to the correlated-errors setting: each time the model reaches the root, it behaves almost as if it is choosing a child uniformly at random, and temporally correlated errors can cause it to revisit the same children and loop.

To understand why looping is weaker here than in Section 4, it is helpful to condition on the model having already visited one wrong child, gone to its leaf, and then returned to the root. At this point, the training distribution still assigns probability 0.5 to the correct child and  $0.5/4$  to each wrong child, but a reasonable learner can now at least tell that the previously visited child is bad. A simple way to model this is to assume that the learner can give the visited child its own probability, while treating the remaining four children (three unseen wrong children plus the correct child) as indistinguishable. Under this constraint, the maximum-likelihood solution puts  $0.5/4 = 0.125$  on the already-visited child and spreads the remaining  $1 - 0.125 = 0.875$  uniformly over the other four children, giving about 0.219 probability to each. In other words, compared to a perfectly uniform  $1/5 = 0.2$  split, the visited child is slightly downweighted, which is very similar to the margin variant from Section 4 with a margin of about 0.075. On top of this effective distribution, the Transformer’s temporally correlated errors once again bias it toward reselecting a few children. Indeed, the looping curves in Figure 14 look very similar to those for margin  $m = 0.1$  in Section 4.

**Inducing more severe looping.** The explanation above also suggests how to induce more severe looping by making the task harder for the student. Consider a  $G(10,5)$  graph. At the root, the teacher places probability 0.5 on the correct child and spreads the remaining 0.5 uniformly over four incorrect children, giving probability  $0.5/4$  to each of these, while never visiting the remaining 5 children. Thus the teacher only ever explores five root children in total. Now condition again on the model having visited one of the wrong children once and returned to the root. A learner that can recognize this visited child as bad, but still cannot distinguish the remaining nine children from one another, will put about  $0.5/4 \approx 0.125$  probability on the visited child and spread the remaining  $1 - 0.125 = 0.875$  uniformly over the other nine children, giving roughly  $(1 - 0.5/4)/9 \approx 0.097$  to each. Under greedy decoding, the model will then prefer the already-visited child at the root and keep returning to it, producing stronger loops. We implemented this variant and include its results in Figure 14; as we expected, it exhibits substantially more looping.

Overall, these instances show that looping similar to Section 4 can occur even when the teacher distribution places significant mass on the correct progress-making action. They also illustrate that the basic principles in this paper can combine in different ways to cause looping; a problem need not match exactly the setups in Sections 3 and 4 for these mechanisms to appear.

## E A CATALYST FOR LOOPING

In looping traces from open reasoning models, we also see another force that acts as a catalyst for looping. At the beginning of a loop, the model’s probability distribution over next tokens looks relatively normal, but as it repeats the same text, it tends to become more and more confident in the looping continuation. This makes it harder for the model to escape once it has been looping for a while.

Figure 15 illustrates this effect. We take two looping traces on AIME 2025 Problem I-7 and Problem I-5, generated with greedy decoding using the OpenThinker3-1.5B model (these traces are also discussed in Examples 1 and 2). For each trace, we plot the highest probability assigned to any next token at each decoding step. The red line marks the step where the final infinite loop begins. As the loop progresses, the maximum probability rises, showing that the model becomes increasingly confident in continuing the loop.

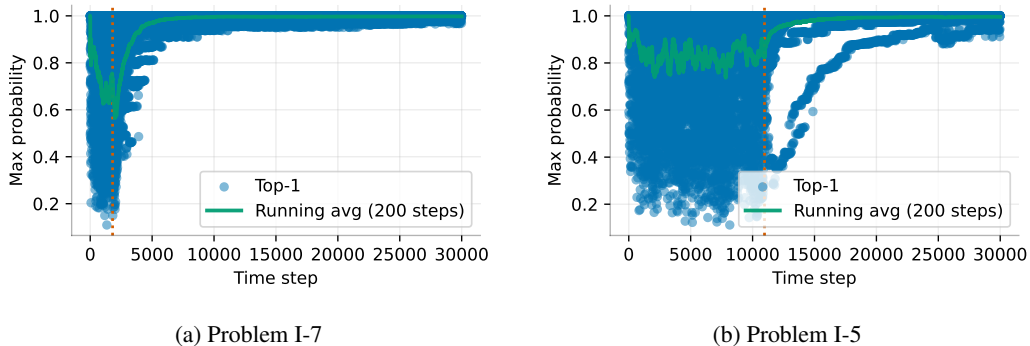


**Figure 15: Confidence buildup during looping.** We plot the maximum next-token probability over time for two looping traces from OPENTHINKER3-1.5B on AIME 2025 Problem I-7 (a) and Problem I-5 (b), generated with greedy decoding. Each blue dot shows the top-1 probability at a single decoding step; the apparent vertical bands are due to plotting 30k time steps at this resolution. The green curve is a running average (window size 200). The vertical dashed line marks the step where the final infinite loop begins. In both cases, once the loop starts, the top-1 probability rises toward 1, indicating that the model becomes increasingly confident in continuing the loop.

### E.1 EXPLICITLY INTRODUCING THE BIAS

In reasoning models, there can be many sources of such a bias. For example, during pretraining the model may see a few sequences where a piece of text is repeated many times. Later, when the model has already repeated itself for a while, the conditional probability of continuing the repetition can become much larger than it was in the original training distribution. We leave a thorough analysis of how this bias arises to future work. Here, we show that a tiny change to the training distribution is enough to introduce such a bias, and that it significantly amplifies the looping mechanisms we discussed.

**Risk-aversion mechanism** We first revisit the risk-aversion mechanism from Section 3. Recall that, due to hardness of learning, the model tends to loop between the start node and the root node. We now modify the training distribution so that, with a very small probability 0.001, the training example is a trace that deterministically loops between the start and root, and with the remaining probability we sample the example as before. Since this looping probability is so small, it does not noticeably change the learned distribution early in a generation. However, once the model has already looped between the start and root for some time, conditioning on this history makes the looping trace much more likely. As a result, the model becomes increasingly confident in continuing the loop.

Figure 16 shows this effect. For 500 model-generated traces with greedy decoding, we plot the probability assigned to the reset (start) action each time the model visits the root. Without the bias, this probability stays around its learned value near the teacher’s 0.3. When we add the bias, the reset

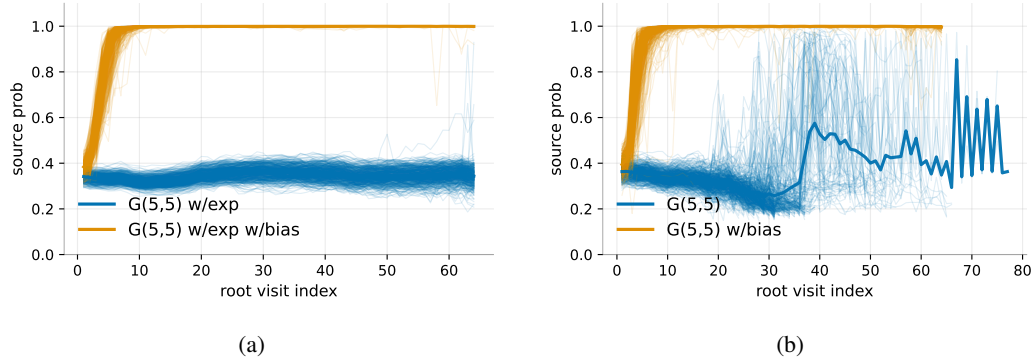


**Figure 16: Explicit looping bias drives reset probability toward 1.** We work in the risk-aversion setting on  $G(5, 5)$  (Section 3), with and without exploration. For each of 500 greedy-decoded traces, we record at every visit to the root the model’s probability of taking the reset-to-start action (“source prob”) and plot it against the root-visit index (thin lines). The thicker lines show the average over all traces that reach that visit index (traces that have already ended are not included in the average). In the biased models (orange), the training distribution is modified so that with probability 0.001 the example is a trace that deterministically loops between start and root, and with the remaining probability it is sampled as before. Under this bias, the reset probability quickly rises toward 1 as the number of visits grows, so once a loop has persisted for a while the model becomes almost certain to continue it. In the unbiased models (blue), the reset probability stays roughly constant in the exploration variant (a) and generally drifts downward in the non-exploration variant (b); the late oscillations in (b) come from a few trajectories that take invalid transitions and revisit the root many times.

probability quickly climbs toward 1 over successive visits, showing that the model becomes nearly certain it should keep looping once the loop has gone on for a while.

Figure 17 reports accuracy, looping counts, and response lengths versus temperature for  $G(5, 5)$  with and without exploration (similar to Section 3), comparing models trained with and without the added bias. With the bias, looping is clearly amplified. For example, on  $G(5, 5)$  without exploration, the original model typically loops between the start and root for a while and then escapes to some root child, reaching an arbitrary leaf; this yields accuracy close to chance under greedy decoding. After adding the bias, once the model has looped for some time, the reinforced reset probability keeps it trapped between the start and the root, and greedy-decoding accuracy drops close to zero.

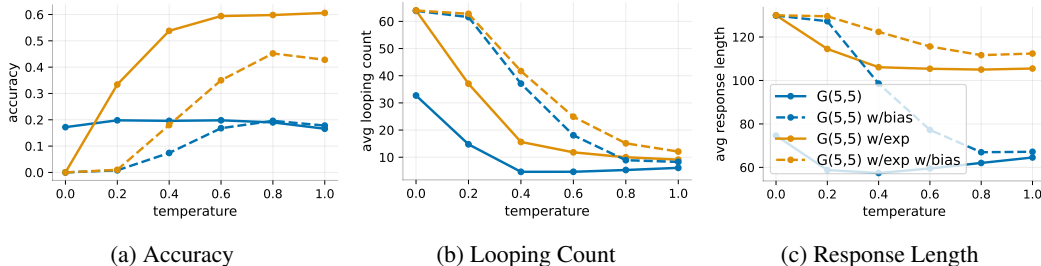


**Figure 17: Confidence bias amplifies looping and degrades accuracy.** In the risk-aversion setting on  $G(5, 5)$  (Section 3), we plot accuracy, looping count, and response length versus temperature, with and without exploration, comparing models trained on the original distribution (solid) and with an added looping bias (dashed). The bias increases low-temperature looping counts and response lengths and, in the non-exploration setting, drives greedy-decoding accuracy close to zero by keeping the model trapped between the start and root once a loop has formed.

**Correlated errors mechanism.** Next we revisit the correlated errors mechanism from Section 4. Here again we introduce a tiny looping bias. With a small probability 0.001, the training distribution

picks a random non-goal leading child at the root (fixed once at the start of the trace) and generates a loop: from the root it goes to that child, walks forward to the leaf, resets to the start, returns to the root, takes the same child again, and so on. With the remaining probability, traces are drawn as before.

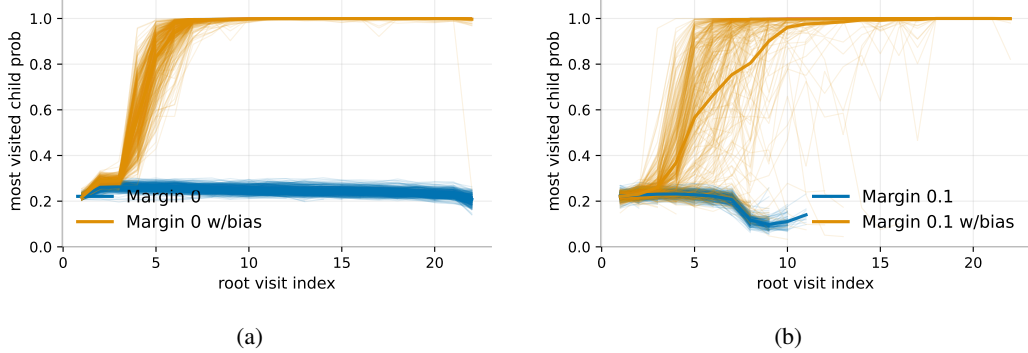


**Figure 18: Explicit looping bias reinforces a single child at the root.** For the correlated-errors setting on  $G(5, 5)$ , we compare models trained with and without an additional looping bias, for margin 0 (a) and margin 0.1 (b). The bias is introduced by modifying the training distribution so that, with small probability 0.001, a trace repeatedly goes from the root to a fixed non-goal child, walks to its leaf, resets, and repeats. For each greedy-decoded trace, we identify the most visited child at the root and, at every visit to the root, record the probability assigned to that child (“most visited child prob”). Thin lines show individual traces; thicker lines show the average over traces that reach each visit index. With the added bias (orange), this probability quickly increases toward 1 as the number of visits grows. In the margin-0.1 setting, some traces leave the loop early, but most traces that loop for a bit become increasingly confident in choosing the same child again. Without the bias (blue), the probability on the most visited child stays roughly flat or drifts downward.

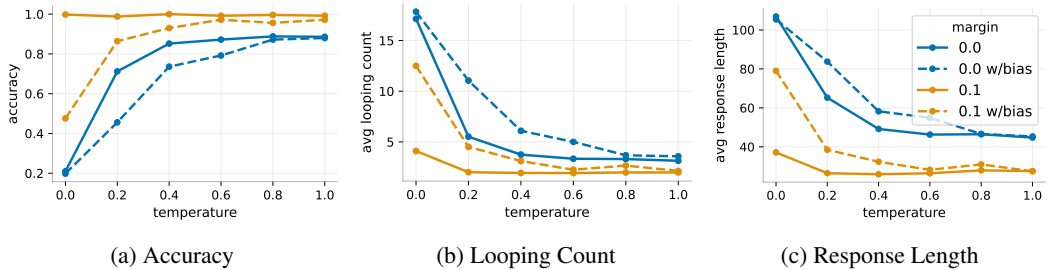


**Figure 19: Confidence bias amplifies looping under temporally correlated errors.** In the correlated-errors setting on  $G(5, 5)$  (Section 4), we plot accuracy, looping count, and response length versus temperature for margin 0 and margin 0.1, with and without an added looping bias. Solid lines use the original training distribution; dashed lines add the bias that occasionally generates traces which always revisit the same non-goal child at the root. The bias increases low-temperature looping counts and response lengths, and decreases low temperature accuracy. The effect is especially significant for the margin 0.1 setting.

As before, this small change amplifies looping. In Figure 18, for each trace we first identify the most visited child at the root, and then plot the probability assigned to that child at each visit to the root. For the margin 0 variant (panel (a)), this probability steadily increases and moves close to 1 when the bias is present. For the margin 0.1 variant (panel (b)), some trajectories leave the loop early, but for those that keep looping for a while, the probability on the most-visited child is again reinforced and rises toward 1.

Figure 19 shows accuracy, looping count, and response length versus temperature, similar to Section 4. Here too we see amplified looping. In particular, for the margin 0.1 setting, we previously

observed only mild looping; with the added bias, looping becomes much stronger and accuracy drops noticeably, especially at low temperatures.